SLAC–PUB–6473
October 1994
(T/E)

A MODEL FOR BALL LIGHTNING*

David Fryberger

Stanford Linear Accelerator Center
Stanford University, Stanford, California 94309

ABSTRACT

A model for ball lightning (BL) is described. It is based upon the vorton model for elementary particles, which exploits the symmetry between electricity and magnetism. The core, or driving engine, of BL in this model is comprised of a vorton-antivorton plasma. The energy of BL, which derives from nucleon decay catalyzed by this plasma, leads, through various mechanisms, to BL luminosity as well as to other BL features. It is argued that this model could also be a suitable explanation for other luminous phenomena, such as the unidentified atmospheric light phenomena seen at Hessdalen. It is predicted that BL and similar atmospheric luminous phenomena should manifest certain features unique to this model, which would be observable with suitable instrumentation.

Invited talk presented at the First International Workshop on the Unidentified Atmospheric Light Phenomena in Hessdalen, Hessdalen, Norway, March 23–27, 1994.

∗ Work supported by Department of Energy contract DE–AC03–76SF00515.

I. INTRODUCTION

While there remain a number of skeptics, it is fair to say that there are sufficiently many sightings of ball lightning (BL) by reliable observers to be generally convincing that BL exists as a natural phenomenon and that it is related to thunderstorm activity; the frequency of BL sightings correlates closely with the diurnal frequency of thunderstorms (mostly in the afternoon) and with the annual frequency of thunderstorms (mostly in the summer). More to the point, BL has been observed to appear directly out of the channel of a lightning bolt.

There are available a number of excellent comprehensive reviews of BL.[1–7] One can find in these reviews catalogues of BL sightings, which go back several centuries, as well as descriptions of numerous theories and models that have been offered as explanations, or partial explanations, of the phenomenon. However, it has proven most difficult to find a persuasive explanation for the salient features of the observed BL, and none of the theories or models that have been offered to date have gained general acceptance. Furthermore, when the BL phenomenon is considered in more detail, one finds that the features and circumstances of the reported BL are so varied that it is often suggested that there may be more than one type of BL.

While most BL sightings have been during thunderstorm activity, it is also true that a significant fraction of the sightings have occurred during periods of (locally) clear weather.[8] These sightings might be somehow related to more distant thunderstorm activity (They still appear to correlate with thunderstorm frequency.) or perhaps to some other source. Going beyond the collections of BL reports, there are numerous reports of other atmospheric luminous phenomena which, as phenomena, intrinsically appear to have much in common with BL, but which are not considered to be related to thunderstorm activity. These other luminous phenomena are often called earth lights,[9] and it has been suggested that they may be associated with various geophysical phonemena: dynamic ones such as earthquakes or volcanoes, or even static aspects such as fault lines or mineral deposits. However, earth lights as a category would also include the atmospheric luminous phenomena that have been reported at locations such as Marfa (Texas) and Hessdalen[10] (Norway) the source for which is

not at all clear. Although it is an intriguing topic, it is a most difficult one, and consideration of source mechanisms for other atmospheric luminous phenomena must be deferred to a later time.

It is the purpose of this talk to give a progress report[11] on a model for the ball lightning phenomenon that offers a possibility to explain not only the salient features of BL, as observed, but also much of the variety in detail, as observed. In addition, it is argued that this BL model can be extended in a natural way to accommodate other atmospheric luminous phenomena. At the same time, however, it must be acknowledged that while the general physical concept of this BL model is in place, it is also true that much work remains to be done on numerous aspects of the model. For example, while some general aspects relating to the generation of BL by a lighting stroke are discussed, a detailed understanding is yet to be achieved.

As an assessment of the utility of a BL model, one can look first at the salient features of BL. As a guide, Uman[12] has proposed as criteria that any valid theory for BL should account for the following features: 1) the constant brightness, size, and shape of BL for times up to several seconds; 2) the considerable mobility of BL; 3) that BL doesn't tend to rise; 4) that BL can enter houses and other structures and can exist within these structures; and 5) that BL can exist within closed metal structures. In addition to these criteria,[13] a prime question that any viable model for BL should address is the source of energy that enables BL to exhibit an extended period of luminosity. Catalyzed nucleon decay, the energy source in this model, appears to offer an answer to this question. As will be seen later, this explanation for the source of BL energy can also be applied to other luminous phenomena.

At the next level of inquiry, one should ask if the putative model (or theory) can accommodate the sizeable dispersion in the observed features that have been reported. For this inquiry, it is useful to utilize the catalogues of data available in the review papers, as well as particular sightings that have certain details reliably reported. From a perusal of these data, one sees that these features include size, shape, structure, lifetime, decay mode, motion, color, color changes, heat, and brightness, as well as (stable) multiple BL geometries. While

there remains a large amount of detailed analysis to do in this area, it is not inconceivable that the answer to this question could also be yes.

It is predicted that BL, as well as earth lights, should exhibit certain features unique to this model, which would serve to distinguish it from other models. Indeed, it is possible that some of these features may have already been observed, and it is fair to say that reports of these observations furnished important motivation for this BL model. While verification of the predicted BL features with suitable instrumentation would be quite a useful step in the substantiation of this model, the ultimate goal is, of course, to achieve enough understanding of BL to produce it in the laboratory. (It is appropriate to remark here that there are already a number of claims of laboratory production of BL, but in general these claims are met with a certain degree of skepticism; these "laboratory BL" generally do not match well with one or another of the salient BL features, *e.g.*, those proposed by Uman.)

II. MODEL

A. Generalities

This model is based upon "new physics," which is not inappropriate, since past efforts to understand BL in terms of known physics have essentially been unsuccessful. Specifically, this BL model is based upon the vorton model for elementary particles,[14,15] which in turn is based on generalized electromagnetism. It was recognized[16] at the turn of the century that one could generalize Maxwell's equations to include magnetic charge and current, as the symmetric partners to electric charge and current. It was later observed[17] (in 1925) that this symmetry was continuous, and that the amount of "mixing" of electricity and magnetism could be described by an angle (called the dyality[18] angle) in the electromagnetic plane. A basic assumption of the vorton model is that dyality symmetry between electricity and magnetism is fundamental; this model for BL exploits this symmetry extensively.

Dyality symmetry is mathematically founded in a two-potential electromagnetic theory[18,19] which recently has been given a more secure theoretical foundation by means of a dyality-symmetric Lagrangian formulation.[20] It is a natural consequence of a dyality-symmetric, two-potential theory of electromagnetism that there be a second, or

magnetic, photon[21] to accompany the conventional, or electric, photon. (This point has recently been clarified.[22]) Hence, allowing theoretical concepts to lead the way, the existence of a magnetic photon and magnetic charge is assumed. A natural extension of this path is that the quantum mechanical vacuum (the Dirac sea)[23] would contain not only the usual (negative energy) particles (*i.e.*, $e, \nu_e, p, n; \mu, \nu_\mu, \Lambda_c, \Lambda$; *etc.*) but also their magnetic analogues. The reason that these analogue magnetic particles have not yet been observed would be that they are very massive.[24]

As a first step in the formation of ball lightning, it is hypothesized that the lightning discharge produces a large number of vorton pairs. Subsequently, a certain fraction of these vortons collect and form what I shall call the *core* of the BL. From BL observations, one can make estimates of the electromagnetic charge and energy that would characterize this core. Calculations indicate that there is enough energy available in the lightning discharge to form such a core. However, due to lack of reliable theoretical calculations (and certainly no experimental data) on multivorton physics, there is significant uncertainty about the details of the production and formation processes, and this area is left for future study.

Through the modeling (in more or less detail) of various aspects of the core, it is argued that the physics of this core can supply the mechanisms that furnish BL, as well as earth lights, their stability, luminosity, dynamics, and extended lifetime. And in this way, it is shown below that this model has good prospects to satisfy all of Uman's criteria as well as answer the question of the source of BL energy. It is also suggested that quantitative variations in the parameters of the core could explain the extensive variations in the observed features of BL as well as those of other luminous phenomena. No other model for BL that I know of seriously broaches this challenging aspect of BL and other luminous phenomena.

B. The Vorton

Since this BL model is based on the vorton, it is useful first to briefly review the structure of the vorton itself. The vorton[14] is assumed to be the fundamental electromagnetic object. At rest, it is most appropriately described using a (right-handed) toroidal coordinate system, (σ, ψ, ϕ),[25] as depicted in Fig. 1. The ranges of the coordinates are: $0 \leq \sigma \leq \infty, 0 \leq \psi <$

$2\pi, 0 \leq \phi < 2\pi$. The size or scale of the vorton (which depends upon the details of its production process, see Sec. II D) is characterized by the radius a, which sets the scale of the toroidal coordinate system, as shown in Fig. 1.

The electromagnetic charge distribution of the vorton is smooth, continuous, and without singularity, much like a classical fluid. This charge distribution, which is spherically symmetric, is described by a charge density

$$q = \frac{4a^3 Q}{\pi^2 (a^2 + r^2)^3}, \tag{1}$$

where Q is given below by Eqs. (2) and (3); q is plotted in Fig. 2. In a quiescent state, this charge distribution is invariant under rotations with respect to the angles ψ and ϕ, and the vorton carries angular momenta L_ψ and L_ϕ associated with (internal) fluxes of this charge (density) along the direction of the ψ and ϕ unit vectors, respectively. Hence, these fluxes, depicted in Fig. 3, are orthogonal. The ψ-flux (along 1_ψ) around the ring of radius a resembles the motion of a smoke ring and results in a poloidal angular momentum; the ϕ-flux (along 1_ϕ) around the z-axis entails the usual angular momentum. A cut-away view[26] depicting the (combined) vorton flux or flow lines is shown in Fig. 4.

L_ψ and L_ϕ are quantized with quantum numbers m_ψ and m_ϕ, respectively, where, by definition, $m_\psi, m_\phi > 0$ (< 0) when the flux is parallel (antiparallel) to the respective unit vectors. These angular momenta, as indicated in Fig. 3, are (by definition) associated with the z-axis of the physical vorton. (Of course, the z-axis of the physical vorton can have any orientation in space. Thus, in general, the vorton can have components of intrinsic angular momenta associated with the x-, y-, and z-axes of a laboratory reference frame, depending upon the orientation of the vorton.) The vorton also carries a (topological) Hopf charge[27] Q_H deriving from the fact that the vorton simultaneously possesses L_ψ and L_ϕ. The vorton is arbitrarily defined to carry $Q_H > 0$ and the antivorton to carry $Q_H < 0$. Since topological charge is conserved, vortons can only be produced in pairs, and after production are stable (although annihilation is possible).

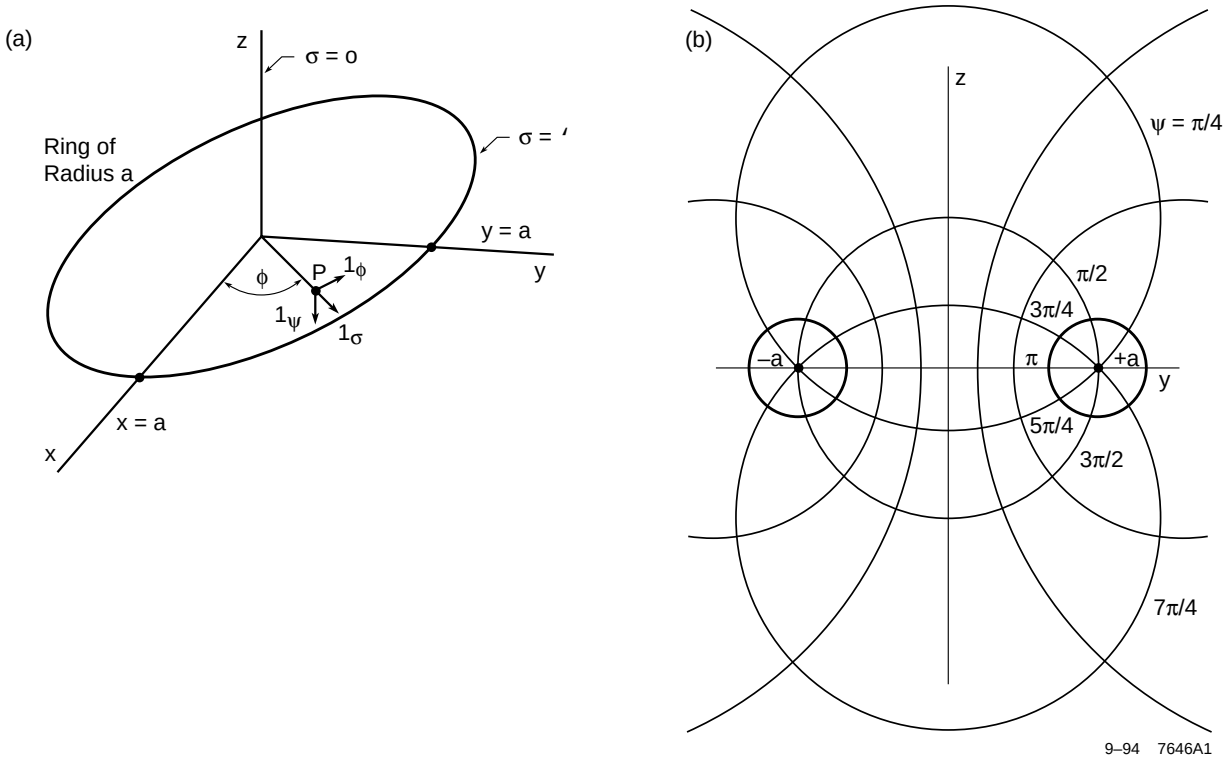

Figure 1. The toroidal coordinate system (σ, ψ, ϕ) has cylindrical symmetry around the z-axis.

a. As indicated, the the z-axis corresponds to $\sigma = 0$ and the ring of radius a in the x-y plane to $\sigma = \infty$. ϕ is the usual (azimuthal) angle of the cylindrical coordinate system. The coordinate system (σ, ψ, ϕ), as shown, is a right handed system; note the depiction of the unit vectors $1_\sigma, 1_\psi$, and 1_ϕ at the point P.

b. Section containing the y-z plane. Surfaces of constant σ are doughnut shaped and circular in cross section, and are nested around the ring of radius a. As shown, cross sections of these tori form nested circles. Surfaces of constant ψ are spheres passing through the ring of radius a, orthogonal to the toroidal doughnuts of constant σ. A cross section of these spheres yields circles in the y-z plane, as shown. The appropriate angle ψ is indicated on the segments of these circles.

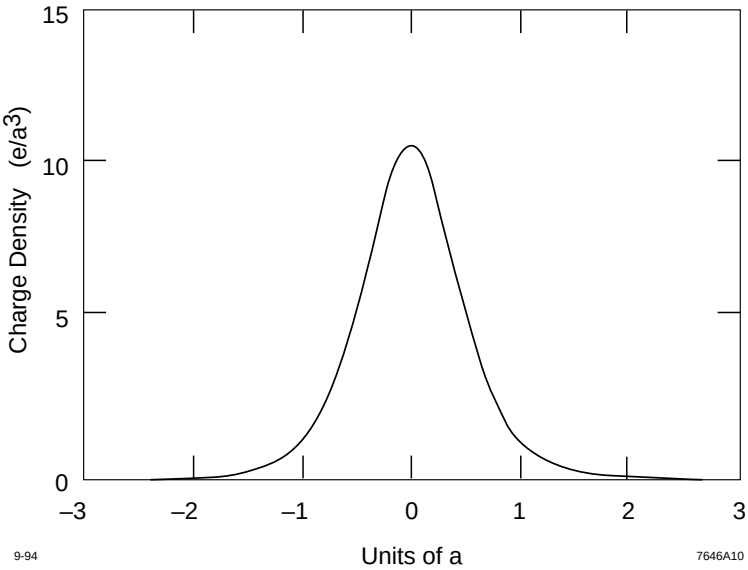

Figure 2. The charge density (in units of e/a^3) of a ground state ($Q = Q_0 = 25.83\ e$) vorton as a function of distance from the center in units of the vorton scale a.

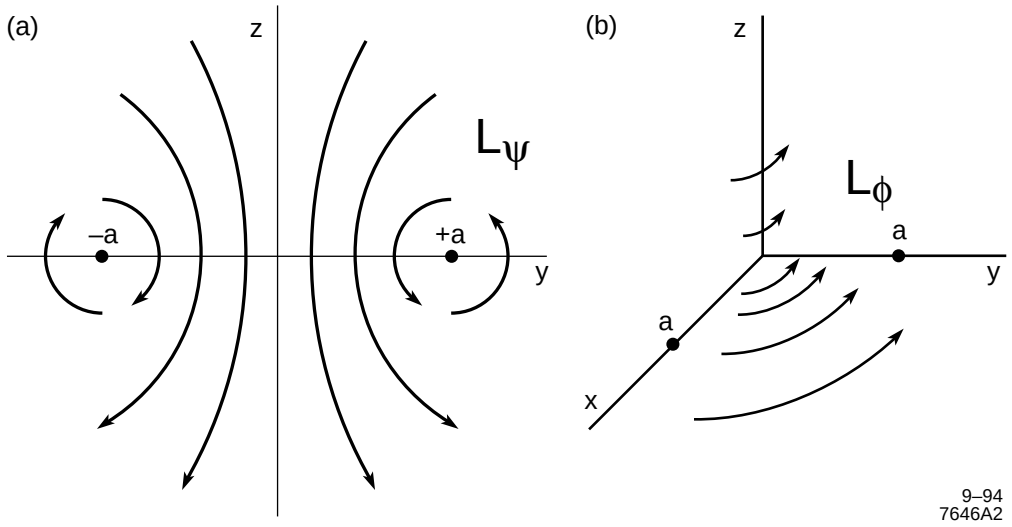

Figure 3. Depiction of flow or flux lines associated with internal vorton circulations.

a. L_ψ is associated with a "rotation" or smoke ring motion along 1_ψ. 1_ψ lies in the surface of a torus of constant σ. L_ψ as depicted is positive; this flow is in the same sense as 1_ψ, as depicted here in the y-z plane.

b. L_ϕ is associated with a rotation along 1_ϕ, that is, around the z-axis. 1_ϕ also lies in the surface of a torus (of constant σ) but is orthogonal to 1_ψ. L_ϕ as depicted is positive; the flow is in the same sense of 1_ϕ.

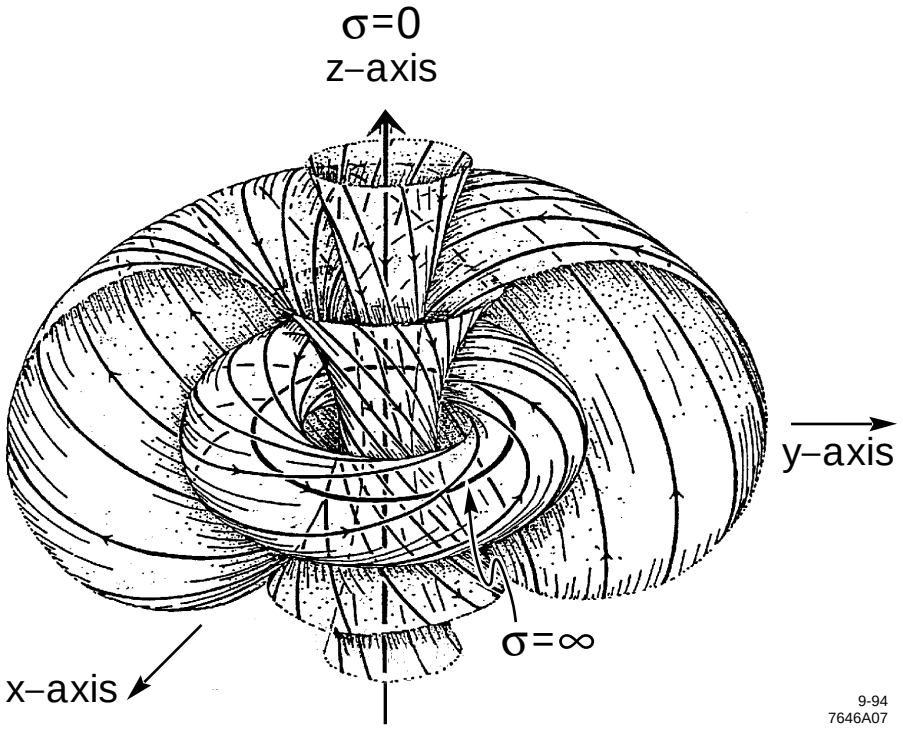

Figure 4. A cut-away view of the vorton charge flux lines that result from combining the ψ-flux and the ϕ-flux. One can see that these flux lines, as indicated by the arrows, all lie in the surface of one of the (nested) tori and are in the sense of increasing ψ and ϕ. (Three rested tori of constant σ, as well as the $\sigma = 0$ line and the $\sigma = \infty$ ring, are depicted here; also, *cf.* Figs. 1a, 1b, and 3.) As discussed in the text, this sense of flux dictates that this configuration would carry a $Q_H > O$. ($Q_H = +1$ when $m_\psi = m_\phi = 1$).

The electromagnetic charge carried by a vorton in its equilibrium configuration, as determined by quantum conditions (independent of a), is of magnitude Q at an arbitrary angle Θ, the dyality angle, where

$$Q^2 = Q_0^2 \sqrt{\frac{m_\psi^2 + m_\phi^2}{2}} \ , \tag{2}$$

and

$$Q_0^2 = 2\pi \sqrt{\frac{3}{5}} \hbar c = 4.867 \ \hbar c \ ; \tag{3}$$

$\hbar$ and c have their usual significance. Q_0 is the minimum or ground state charge (which state satisfies $Q_H = \pm 1$ and $|m_\psi| = |m_\phi| = 1$) and is equal to 1.24×10^{-8} esu or 25.83 e, where

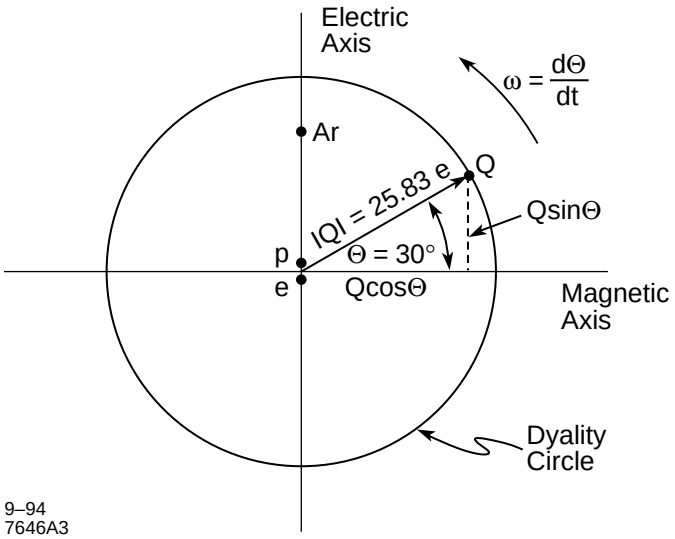

Figure 5. The electromagnetic or dyality plane with electric and magnetic axes is shown. The circle of radius Q_0 (equivalent to 25.83 e), the magnitude of the (ground state) vorton's generalized electromagnetic charge, is also shown. This circle is called the dyality circle. Any point on this circle, designated by its dyality angle Θ, is a possible value for the vorton charge. A $Q = Q_0$ at $\Theta = 30^\circ$ is indicated. For orientation, the electron e, the proton p, and the argon nucleus Ar ($Z = 18$) are plotted. If the vorton is in a state of dyality rotation of angular velocity ω, then $\omega = d\Theta/dt$, as depicted in the figure.

e is the positron charge. It is particularly convenient to use Gaussian units when dyality symmetry is relevant; $\epsilon_0 = \mu_0 = 1$ in Gaussian units, and esu can consequently be used as units for magnetic as well as electric charge. Hence, I shall (usually) use esu as the unit of length for the magnitude of Q in the electromagnetic or dyality plane. Using the angle Θ, the electric and magnetic components of the vorton charge are given by $Q\sin\Theta$ and $Q\cos\Theta$, respectively, as shown in Fig. 5.

Using the Einstein relationship, the mass for the single vorton configuration[14] is

$$M = E_{em}/c^2 = \frac{5Q^2}{2\pi a c^2}, \tag{4}$$

where E_{em} is the electromagnetic energy content of the vorton.

C. Dyality Rotation

After the concepts vortons and vorton production are entertained, dyality rotation, *i.e.*, a rotation of electromagnetic charge in the dyality plane (as depicted in Fig. 5), is perhaps the most difficult physical concept employed in this model; its confirmed existence would add an entirely new phenomenon to known physics. On the other hand, it is a concept that follows quite naturally from the dyality symmetry of Maxwell's equations. For this concept to be physically feasible, it is necessary that photons (actually, for the purposes of this model, both electric and magnetic photons) have a nonzero mass and hence a finite Compton wavelength $\lambda\!\!\!^{-}_{\gamma}$, which defines the range of the electromagnetic interaction. A finite $\lambda\!\!\!^{-}_{\gamma}$ permits the nonconservation of electromagnetic charge.[28]

While it is convenient to assume that the photon is massless, there is no compelling theoretical basis for such an assumption. And from an experimental point of view, it is only known that the photon mass is very small.[29] Given the assumption of a nonzero photon mass, it is legitimate to view the angle Θ as a vortonic degree of freedom; the angular velocity of dyality rotation is simply $\omega = d\Theta/dt$. Θ, as a degree of freedom, has as a conjugate variable the angular momentum L_d. (The subscript d stands for dyality.) The concept of dyality rotation is explored in Appendices A, B, and C.

Later, I will show that dyality rotation plays a key role in the dynamics of this model for BL. It furnishes the mechanisms that enable BL coherence (overcoming Coulomb repulsion), extended BL lifetimes (acting as a kind of "flywheel"), and the source for BL energy (catalyzed nucleon decay).

D. Vorton Production

It is proposed that the production of vortons[30] (in vorton-antivorton pairs), that in this model comprise the BL core, takes place through the mediation of "orphaned" magnetic fields associated with lightning discharge currents. To see how this mechanism would operate, let us first consider the lightning discharge current. The current (vector) of a return stroke is schematically depicted in Fig. 6 as flowing upward along the z-axis;[31] the (azimuthal) magnetic flux loops generated by this current, and which circle the z-axis, are also shown.

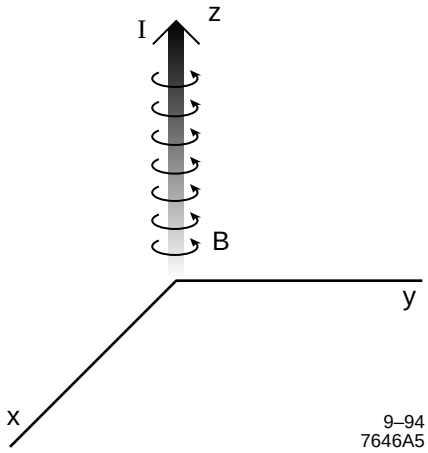

Figure 6. The current of a lightning return stroke is depicted flowing upward along the z-axis. Around this current are shown the closed loops of magnetic flux that it generates.

While the lightning current is depicted to be along the z-axis, it is clear that any orientation of the current flow vector is possible. (Also, we know that the lightning discharge current does not flow in a straight line, but there is no need to include here this bit of realism.)

As the ions and electrons that comprise this discharge current recombine during the course of the lightning discharge, the magnetic fields that they were generating are left abruptly, or orphaned, in space without a source. (Such recombination doesn't take place in metal conductors. Hence, there are no orphaned fields in metal conductors, and the vorton creation process described below is not expected to happen.) Rather than being radiated away, as one would conventionally expect,[32] it is postulated that some fraction of this magnetic field energy will convert into vorton-antivorton pairs *in situ*, the point being that a distribution of suitably oriented vorton-antivorton pairs (with $\Theta = \pm\pi/2$, *i.e.*, electric vortons) will give a magnetic field with the same topology and general shape as that generated (and orphaned) by the original lightning current. To best duplicate, or replace, the (orphaned) magnetic fields of the lightning current, these (created) pairs will all be oriented to have an upward flowing (poloidal, *i.e.*, parallel to 1_ψ, actually -1_ψ) current along the z-axis. Hence, as does the lightning current, the created vortons will have an azimuthal magnetic field circulating around the z-axis due to the sum of their poloidal currents. (This production geometry easily generalizes to more realistic lightning current

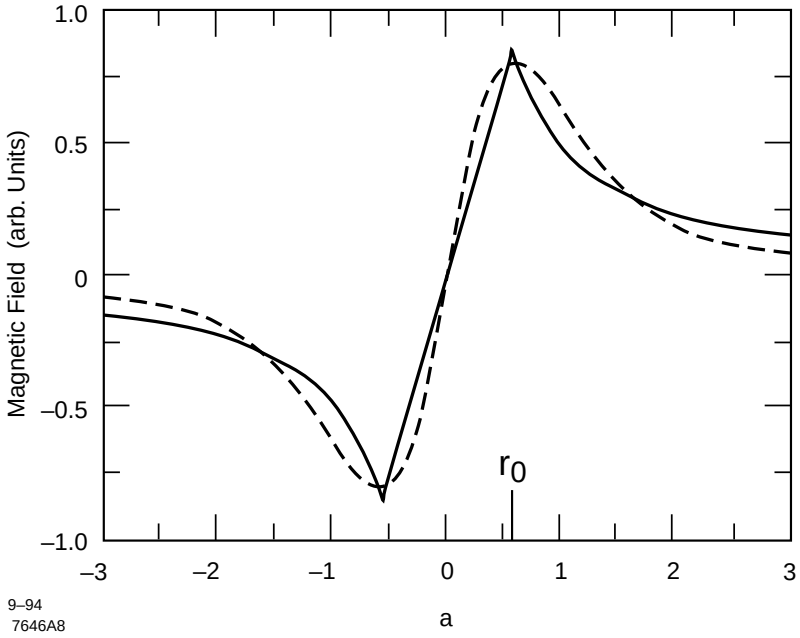

Figure 7. Comparison of the field of a lightning current (solid line) to the azimuthal vorton magnetic field (dashed line). The lightning current has a uniform current density out to a radius r_0, and the vorton field is in the x-y plane of a vorton as shown in Fig. 4. The fields, as plotted here, reverse in sense at the origin because the positive direction for the magnetic field plot is taken to be into the plane of the paper (rather than along 1_ϕ).

flow patterns.) One would expect that the vorton pairs that are generated in this orphaning process will be distributed fairly uniformly along the lightning discharge channel[33] with their z-axes parallel and in close proximity to the (local) channel centerline.

Since the vorton configuration of electromagnetism does not have an intrinsic scale,[14] the shape and size of the orphaned magnetic fields will determine the scale and locations of the vorton pairs that are formed by this process, the vorton pairs making a "best fit" (to some extent analogous to a Fourier expansion of an arbitrary function) to the shape of the orphaned electron and ion fields. To give an idea of the similarity in shape exhibited by a vorton field and the field of the lightning discharge, the magnitude versus radius of the azimuthal magnetic field of a current channel of uniform current density is shown in Fig. 7, along with an azimuthal vorton field of approximately the same scale.

From this discussion, and looking at Fig. 7, one can see that the radius of the lightning discharge channel will set the scale of the produced vortons at $a \sim 2r_0$. However, to derive an estimate for a from knowledge about the radius of the lightning discharge is somewhat problematical. In the first place, estimates of channel radii based upon experimental data vary considerably[34]—from millimeters to over 10 cm. This problem is further complicated by the fact that lightning channels expand very rapidly due to the local heating by the lightning current. (The pressure in the channel has been estimated to be on the order of 10 atmospheres.)[34] There is also the question of the timing of the orphaning production process with respect to the current flow waveform of the lightning discharge process. Earlier times, which would be characterized by smaller diameters and the greatest currents, charge densities, and temperatures, would be the most relevant for this model; since recombination proceeds more rapidly where there is more ionization (*i.e.*, more current density), vorton production would be expected to peak roughly when and where the current densities are maximum, that is, early in the return stroke current waveform.[35] On this point, the measurement of channel radius by means of radar, which is most sensitive when the electron density is the highest, is perhaps the most relevant experimental number; Holmes *et al.*[37] deduce ~ 1 cm as the radius of the lightning discharge channel using a radar technique.

A numerical calculation of the various processes that take place in and near the lightning return stroke channel has been performed,[36] and this calculation is in reasonable agreement with experimental data. These calculations use a current waveform that peaks at 5 μs (somewhat later than the model of Lin *et al.*[35]), at which instant the calculated lightning channel extends out to a radius of ~ 0.5 cm. Therefore, considering these results, it appears reasonable to use $a = 1$ cm for the purposes of calculation. (It is also appropriate to observe that $a = 1$ cm is easily compatible with a mean BL diameter of 19 cm[38] and, in fact, is not in a serious conflict with the smallest reported sizes of BL, which are on the order of a centimeter.[38])

As outlined above, then, it is assumed that some fraction of the orphaned magnetic fields will convert into the azimuthal magnetic fields of vorton pairs, that is, into vorton pairs. Two such pair arrangements are shown in Fig. 8. In a state of complete overlap at production, these pairs will have no other electromagnetic fields. For these pairs, being composed of

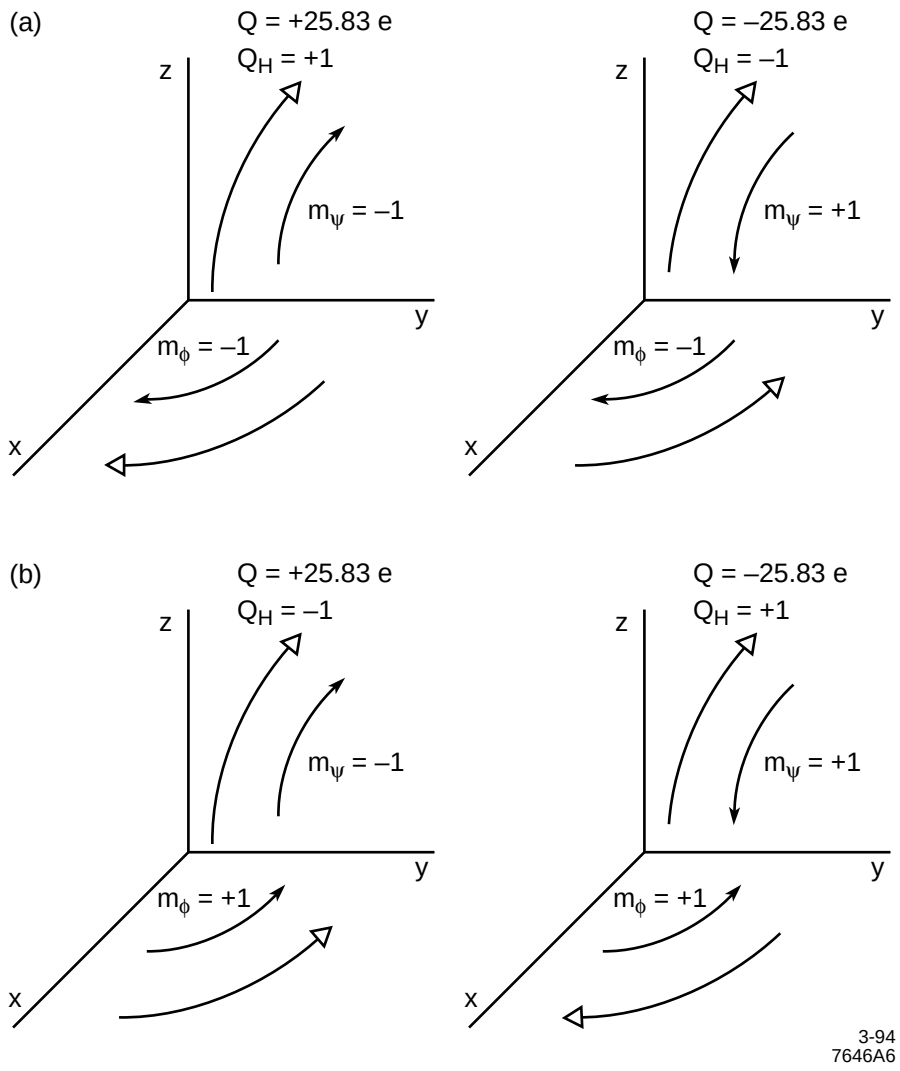

Figure 8. The internal flux patterns for two distinct vorton-antivorton pairs are depicted. The directions of the ψ and ϕ fluxes are indicated by solid arrows, and the accompanying current flow lines by hollow arrows. The dyality angles of the vortons in these pairs are in the electric direction, $\pm\pi/2$, as implied by the indicated charges. Both pairs will give an azimuthal magnetic field in the same sense as indicated in Figs. 6 and 7. All of the other vorton fields of these pairs (both electric and magnetic) cancel after summation.

a. Pair configuration with Q_H and Q of the same sign.

b. Pair configuration with Q_H and Q of opposite sign.

vortons of opposite charge, the static electric charge distributions will exactly cancel—thus, no (initial) electrostatic field. It also follows that for such a pair configuration, the poloidal (dipole) magnetic fields due to the sum of the azimuthal currents will also (initially) cancel. The portion of the originally orphaned magnetic field (energy) that the vortons do not accommodate will then radiate away.

E. BL Charge and Energy Content

It is straightforward to estimate (a range for) the magnitude of the electromagnetic charge in the core of a BL using reports of magnetic effects associated with BL. In one case,[39] a BL influenced the magnetic and radio compasses of a Russian aircraft flying over Irkutsk. In a similar report,[40] in which a BL collided with an aircraft, the radio compass rotated and the magnetic compass spun erratically for 3–5 minutes after the event. If we now assume that in these cases, the BL (core) produced a magnetic field of 2 G (the field would have to be somewhat larger than the earth's field) at a distance $\ell = 10$ cm, then the total (magnetic) BL charge estimate is $Q_{TOT} = B\ell^2 = 200$ esu(equiv). In another case, involving the bell of a church steeple, it was estimated[41] that there was a magnetic field from the BL of 150 G which inhibited the motion of the bell. In this case, using a distance of 12 cm and the estimated 150 G figure, yields $Q_{TOT} = 2 \times 10^4$ esu(equiv). Using these figures, one obtains an estimate for the (range of) charge in the BL core:

$$Q_{TOT} = 2 \times 10^{3\pm1} \text{ esu(equiv)} \sim 7 \times 10^{-7\pm1} \text{ C}. \tag{5}$$

In view of the uncertain nature of these estimates for the magnetic field, this result isn't particularly precise, but at least it's a place to start.

Using this value for Q_{TOT} and data from BL observations, it is possible to estimate the energy content E_{BL} of the core of BL. It is simply

$$E_{BL} = \frac{Q_{TOT}^2}{\bar{r}_{BL}}, \tag{6}$$

where the radius $\bar{r}_{BL}$ typifies the size of the BL core charge distribution. For $\bar{r}_{BL}$, we can use the mean observed value for BL diameter as determined (statistically from a log-normal

distribution) by Dijkhuis.[38] Thus, $\bar{r}_{BL} = (1/2)\bar{d}_{BL} = (1/2)$ (19 cm) = 9.5 cm, which, using Eqs. (5) and (6), gives an estimate for the range of BL energy content:

$$E_{BL} = 4 \times 10^{5\pm2} \text{ ergs} = 4 \times 10^{-2\pm2} \text{ J}. \tag{7}$$

This value is far short of the estimated energy yields of BL,[7] but, as will be described later, this core intrinsic energy is not the source of the energy released by the BL phenomenon. Hence, the magnitude of E_{BL} given by Eq. (7) does not pose a problem for this model.

It is of interest to use Eq. (5) and the value of Q_0 given by Eq. (3) to estimate the number of vortons N_v in the core of a BL:

$$N_v = \frac{Q_{TOT}}{Q_0} = \frac{2 \times 10^{3\pm1}}{1.24 \times 10^{-8}} = 1.6 \times 10^{11\pm1}. \tag{8}$$

This result is based upon an assumption that the quantum condition for Q_0 is unaffected by the vorton interaction energies, which in the BL configuration will considerably exceed the self-mass energies.[42] However, even if the actual Q and N_v differ substantially from the above values, we would still be working with the same Q_{TOT}, and the estimate given in the next section indicates that there is sufficient (local) energy in a lightning discharge to create the core of a BL of the general description contemplated here—even if the vorton pair generation process is not particularly efficient. In addition, deductions concerning the general or global features of BL in this model would not be significantly modified by the BL being composed of fewer but heavier and more highly charged vortons.

F. Energy Available for BL Production

In this model, it is proposed that the magnetic energy of the lightning discharge converts into the vortons that comprise BL. To explore this idea, we estimate the magnetic field and the consequent magnetic energy density associated with a typical lightning stroke and then compare this energy to that of Eq. (7), above. For this purpose, let us assume that we have a uniform current density i flowing in a channel of radius r_0. (One might try to use a more

realistic distribution for i, *e.g.*, a Gaussian, but such a refinement is not warranted at this stage.) In this case, total current in the discharge channel

$$I_c = 2\pi \int_0^{r_0} i \; r dr = \pi r_0^2 i. \tag{9}$$

For $r < r_0$, the magnetic field

$$B = \frac{\mu_0 r i}{2} = \frac{\mu_0 r I_c}{2\pi r_0^2}, \tag{10}$$

where $\mu_0 = 1.26 \times 10^{-6}$ H/m is the permeability of free space. (Rationalized mks units are employed here for convenient use of data on lightning discharges.) For $r > r_0$,

$$B = \frac{\mu_0 I_c}{2\pi r}. \tag{11}$$

Using the magnetic energy density, given by $\frac{B^2}{2\mu_0}$, yields the energy stored along a current flow of length L:

$$W_c = \frac{L\pi}{\mu_0} \int_0^{\infty} B^2 r dr \tag{12}$$

$$\cong \frac{L\pi}{\mu_0} \Big\{ \int_0^{r_0} \Big(\frac{\mu_0 r I_c}{2\pi r_0^2} \Big)^2 r dr + \int_{r_0}^{\hat{r}} \Big(\frac{\mu_0 I_c}{2\pi r} \Big)^2 r dr \Big\}, \tag{13}$$

where (to eliminate a logarithmic divergence) $\hat{r}$ is taken as a radius beyond which we assume the conversion (efficiency) of orphaned magnetic field energy into vortons drops to zero. For convenience in evaluating Eq. (13), it is assumed that $\hat{r} = 5.755 \; r_0$. (The result is not particularly sensitive to this assumption; $\hat{r}$ enters only as an argument of a logarithm.)

Looking at Fig. 7, we see that this value of $\hat{r}$ implies that the region of active conversion into vortons extends out to about three vorton radii. Thus, Eq. (13) reduces to

$$W_c = \frac{\mu_0 L I_c^2}{2\pi}. \tag{14}$$

This energy can be equated to the deduced BL energy (divided by η_{vp}, an assumed energy conversion efficiency for this vorton production) to yield the necessary (minimum) lightning discharge length needed to create a BL. That is,

$$L_{min} = \frac{2\pi E_{BL}}{\mu_0 I_c^2 \eta_{vp}}. \tag{15}$$

Taking $I_c = 10^4$ A,[34] $E_{BL} = 4 \times 10^{-2}$ J, the central value of Eq. (7), and $\eta_{vp} = 1$ (for the sake of argument), yields

$$L_{min} = 2 \times 10^{-3} \text{ m}. \tag{16}$$

An estimate for η_{vp} can now be obtained by assuming that the relevant discharge length for BL production is approximately 0.19 m, the mean BL diameter.[38] In this way, we estimate

$$\eta_{vp} \sim \frac{2 \times 10^{-3} \text{ m}}{1.9 \times 10^{-1} \text{ m}} \sim 10^{-2}. \tag{17}$$

Thus, it appears plausible that the lightning discharge can generate in one locale enough vortons for a BL core; the conversion efficiency of magnetic energy into a BL needs to be $\sim 1\%$. Actually, η_{vp} could be an order of magnitude (or more) below this figure if it is only the most powerful lightning strokes that generate BL. These have currents that exceed by more than an order of magnitude[34] the 10^4 A used to obtain Eq. (17).

G. BL Core Physics

1. General Remarks

In general terms, once formed,[43] the core of the BL has a well-defined physical description (which description could also apply to other atmospheric luminous phenomena) much like a plasma, but with important additional features. It is comprised of macroscopically-sized vortons and antivortons with significant spatial overlap and with electromagnetic charges in a state of coherent dyality rotation. This core is the driving engine that leads to the various observed features of BL as a phenomenon. For example, core mechanisms give the BL a spatial coherence and longevity that is not achievable in other models [especially if one undertakes to explain the observed (greater than) one hour lifetime of (some of) the Hessdalen lights]. In this model, the primary parameters which would characterize the core of an individual BL are N_v and L_d; there are numerous secondary parameters, some of which, in principle, should be derivable from N_v and L_d. Other luminous atmospheric phenomena, *e.g.*, the Hessdalen lights, will also fit this prescription, but presumably with larger values for N_v and L_d.

2. Equilibrium Point

It is shown in Appendix B that as a consequence of dyality rotation in a BL, there will exist attractive forces between like charged vortons, opposing the usual Coulomb repulsion. These forces are strong enough, in fact, that there is a point of stable equilibrium for the BL configuration. Eq. (B-6), which shows the trade-off in BL energy between the static E_c and the dynamic E_d, is schematically depicted in Fig. 9. The equilibrium point A is indicated at the minimum of the curve $E_{tot} = E_c + E_d$. At this equilibrium point,

$$E_c = E_d, \tag{B-7}$$

and the angular velocity (or frequency) of the dyality angle

$$\omega = \sqrt{2}c/(k\overline{\lambda}_\gamma) \equiv \omega_0, \tag{B-8}$$

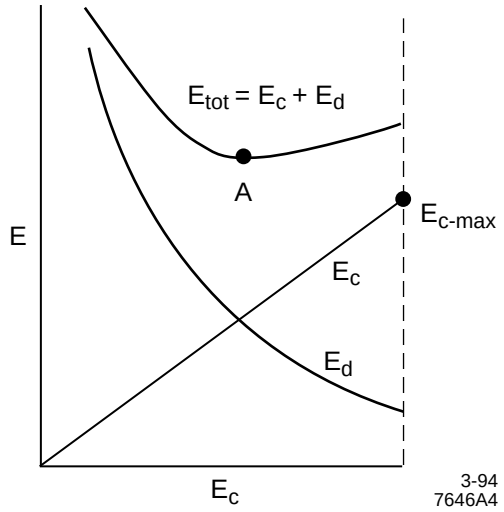

Figure 9. Depiction of total vorton energy $E_{tot} = E_d + E_c$ as a function of E_c. The point of stable equilibrium A is shown. E_{c-max}, the maximum value for E_c ($r_{BL} = \bar{a}$), as described in the text, is also indicated.

where the most recent results[29] for λ_{γ_e} (and assuming $k = \sqrt{2}$, for convenience) give $\omega_0 \lesssim 1\ s^{-1}$. The existence of this stable equilibrium point is important, for it furnishes the BL of this model a mechanism for coherence and long lifetime. It is interesting to observe that these results are independent of the number of vortons in the BL as well as of E_c, E_d, and L_d. ω_0, then, being dependent only on the speed of light and $\overline{\lambda}_\gamma$, the Compton wavelength of the photon, is a fundamental physical constant.

3. Equilibrium Frequency

It is useful to explore further the physics of this equilibrium point and find a more general expression ω_{eq} for the equilibrium (angular) frequency. As one imagines a BL of some specified N_v endowed with a larger and larger L_d, the appropriate E_d curve in Fig. 9 will lie higher and higher. This causes the equilibrium point to shift to the right, as the E_c required for equilibrium would also increase. But still $E_c = E_d$ and $\omega_{eq} = \omega_0$ would be maintained. However, this compensation (equal division of energy) cannot continue indefinitely; for a sufficiently high L_d, E_c (and hence also I_d) will be at its highest allowed value, which occurs at $r_{BL} \cong \bar{a}$ (the mean vorton size in the BL). At this point, the vortons will be in full

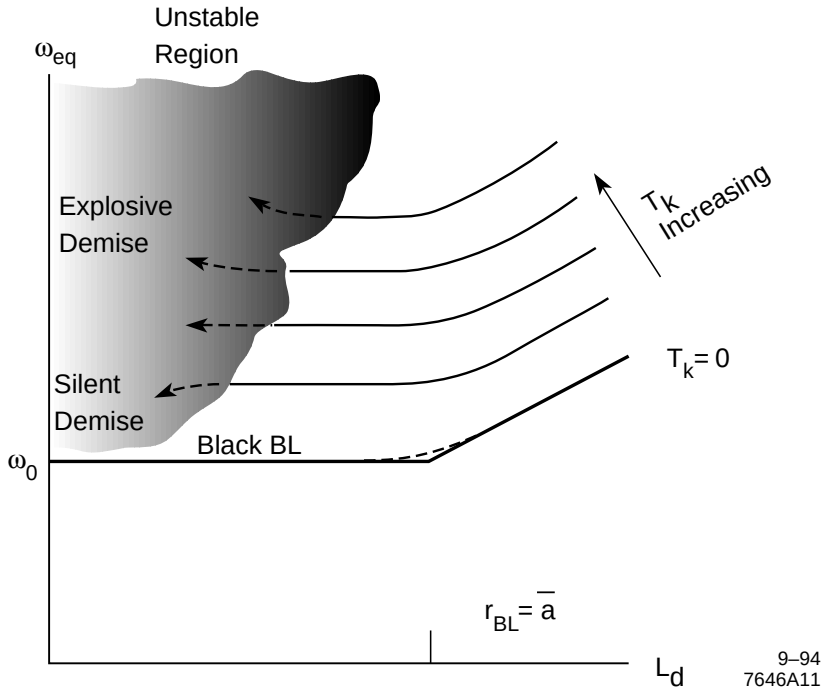

Figure 10. A family of ω_{eq} curves as a function of the variable L_d and the parameter T_k. The lowest curve (heaviest line) has $T_k = 0$ and shows that $\omega_{eq} = \omega_0$ as $L_d \to 0$. For $T_k > 0,\ \omega_{eq} > \omega_0$. Several curves for increasing T_k are indicated with lighter lines. These curves do not extend down to $L_d = 0$ because the kinetic gas pressure will cause the BL to disintegrate for low L_d. The conjecture about possible decay paths toward silent demise (smaller T_k) or explosive demise (larger T_k) are dashed in at the small L_d end of the curves where a region of instability is indicated.

spatial overlap and with fully coherent Θ_i. Beyond this point, as the L_d is increased, ω_{eq} must rise linearly, in proportional to L_d ($\omega_{eq} = L_d/I_d$). These relationships are depicted in Fig. 10; the lowest curve, starting at ω_0 for $L_d = 0$, is the $T_k = 0$ curve. (T_k is a kinetic temperature to be described shortly.) A dashed line is sketched in to suggest a smoother transition between the flat and linear regions.

With this discussion of the $T_k = 0$ curve as background, we can now refine the analysis for the equilibrium frequency by taking into account the random motions of the individual vortons (and coherent groups of vortons) with respect to the center of momentum of the BL. Assuming that the N_v vortons constitute an ideal gas at thermal equilibrium at a temperature

T_k, one can calculate the total energy E_k in the (translational) degrees of freedom of the vortons in a BL:

$$E_k = N_v n_k k_B T_k/2, \tag{18}$$

where n_k is the number of (active) degrees of freedom[44] per vorton and k_B is Boltzmann's constant. E_k is a form of heat which would derive from the primary BL energy source, catalized nucleon decay, to be described later in more detail.

It is shown in Appendix C that one doesn't need to know details about Eq. (18) to obtain useful results. In simple conceptual terms, this vorton kinetic energy generates an internal pressure in the BL that prevents E_c from rising to equal E_d. This result is quantified in Appendix C:

$$\omega_{eq} = \omega_0[1 + 3(\gamma - 1)E_k/E_c]^{1/2}, \tag{C-9}$$

where γ is the ratio of the specific heats of the BL as a vorton gas. Since $\gamma > 1, \omega_{eq} \geq \omega_0$, the equality applying when $E_k = 0$. Thus, as depicted in Fig. 10, one expects a family of ω_{eq} curves above the $T_k = 0$ base curve.

The fact that there are ω_{eq} curves that lie significantly above ω_0 is an important condition for BL luminosity. Also, these curves can be viewed as (approximations to) BL decay trajectories, to be described in Sec. II G 12.

4. Lifetime

With the condition for BL stability in place, the possibility of an extended lifetime for BL (as well as for other atmospheric luminous phenomena) follows in a staightforward way. To visualize this, it is useful to view L_d and E_d as the angular momentum and energy of a "dyality flywheel." The flywheel analogue is apt because of the rotation and because the L_d and E_d loss mechanisms being relatively weak, would permit the flywheel to "turn" for an extended period of time. As a consequence, the longevity of a given BL will be a function of its initial L_d and E_d in this flywheel and can vary over a wide range. This possibility is consistent with observation. For example, taking the mean lifetime of BL to be 7.9 seconds,[38] then the 1.3 min observed[45] duration is $\sim$ 10 mean lifetimes. At the tails of

the distribution, there are reported BL sightings of even longer durations,[38] even as long as 15 min.[46] And it should also be mentioned that if the Hessdalen lights[10] are (essentially) the same phenomenon as BL (as is proposed here), their duration of sometimes over one hour also needs to be accommodated by the model; this requirement would pose a major difficulty for other models. But in this model exceptionally long lifetimes are due to (sufficiently) large initial L_d and E_d. Thus, even the very long-lived Hessdalen lights can be accommodated in a natural way.

5. Primary Energy Source

The primary energy source in this model is the energy released by catalyzed nucleon decay. This nucleon decay results from perturbations to the nucleon wave functions; these perturbations are the direct result of the dyality rotation of the electromagnetic charge of the BL.

As background information to enable a better visualization of this process, we observe that in the vorton model, the elementary fermions are comprised of vorton pairs.[14] The quantum numbers of fermions that distinguish one particle type from another derive from the specific internal structure of the angular momenta (helicities) of the paired vorton state (*i.e.*, the fermion). In this model, since baryon number and lepton number are not absolutely conserved quantities, nucleon decay is possible. The conversion of a proton (quark) to a positron can be effected by a perturbation of the orientation of the angular momenta of the constituent vortons of the pair. Under normal circumstances, however, conversion between baryons and leptons does not take place because the fermions are (meta)stable eigenstates, respecting a symmetry of the fundamental Lagrangian.

A well-known metastable state that can be cited as an analogue to this BL physics is the 2S state of the hydrogen atom, which is forbidden to decay by one gamma emission, but which by two gamma emission decays to the 1S state, but with a lifetime of 1/7 s. By contrast, the 2P $\rightarrow$ 1S (one gamma) transition (releases the same energy but) has a lifetime of 1.6×10^{-9} s. A small local electric field will break the symmetry of the hydrogen wavefunction, mixing a small amount of the 2P state into the original 2S state. This perturbative mixing leads to a rapid 1γ decay of the "impure" 2S state to the lower energy 1S state.[47] The analogy in

this BL model would be a proton to positron or a neutron to antineutrino decay induced by dyality perturbations to the original nucleon wavefunction.

When a large number of (BL) vortons is present, creating a "rotating" electromagnetic field, the dyality angle Θ_0 of the particles comprising the vacuum (Dirac sea),[23] which serves as a reference for material particles, undulates.[48] If the driving frequency is high enough, then the nucleons in its presence will not be able to maintain dyality alignment with the local vacuum reference. This misalignment will result in a perturbative mixing of the local (positive energy) elementary particle eigenstates, which, in turn, will lead to a finite transition probability between elementary particle eigenstates (where allowed by energy conservation).

Of course, in this picture, any $\omega > 0$ would presumably lead to a nonzero transition probability, but the "threshold" frequency marking the effective onset of the nucleon decay regime would be expected to be at $\sim c/\lambda\!\!\!^{-}_{\gamma}$ or on the order of ω_0 as given by Eq. (B-8). In any case, there will be some frequency $\bar{\omega}_0 \sim \omega_0$ that defines an empirical threshold above which catalyzed nucleon decay becomes significant. Thus, the criterion for BL energy generation and hence BL luminosity becomes

$$\omega_{eq} > \bar{\omega}_0, \tag{19}$$

where we can tentatively take $\bar{\omega}_0 = \omega_0$, although refinements in the definition of this empirical threshold are to be expected as understanding of this model improves. It is clear, of course, that when ω_{eq} is larger, the nucleon decay probability and, hence, the BL luminosity will be larger.

When $\omega_{eq} > \bar{\omega}_0$, then, the following general reaction is predicted:

$$v + N \rightarrow v + \bar{\ell} + n\pi + mK, \tag{20}$$

where N stands for nucleon (neutron or proton), $\bar{\ell}$ stands for an antilepton (neutral or charged), π (K) indicates a pion (kaon), and n (m) the number of pions (kaons). (Q_H of the baryon is equal to the Q_H of the antilepton; thus, Q_H is conserved.) The vorton, v, is symbolically included on both sides of the equation to signify a (kind of) catalysis reaction.

The branching ratios of these catalysis reactions of nucleon to specific lepton types (e or μ) is a question for experiment to decide. However, one presumes that e^+ and $\bar{\nu}_e$ would be preferred since (we believe) they are of the same generation (the first) as the proton and neutron. As will be seen later, e^+, being ultra-relativistic, is a much better candidate than μ^+ for heating the BL core.

It is important to observe that the decaying nucleons that participate in this process and furnish the BL energy are to be found in the nuclei of the atoms in the air (or other material, *e.g.*, glass when a BL penetrates a window) at the location of the BL. Details of these nucleon decays, which would be expected to occur inside of nuclei, and the associated nuclear reactions are explored in Appendix D.

6. Core Heating

We can see that the energy that is made available in the nucleon decay processes, represented by Eq. (20), is almost the full mass equivalent of the decaying nucleon or ~ 1 GeV per decay.[49] A significant fraction of this energy is expected to transfer into the degrees of freedom of the BL core, heating the core.

In this model, there are two important thermal reservoirs for core heat:[50] 1) kinetic energy of vorton motion, characterized by the temperature T_k (already discussed); and 2) deformation or strain energy of the (individual) vorton charge distributions characterized by the temperature T_s (to be discussed). Since the dividing line between the phenomenology of these reservoirs is the mean vorton size $\bar{a}$, it is to be expected that energy from the latter reservoir would be generating the visible blackbody radiation discussed below.[51] However, as we shall see, the kinetic vorton motion plays a crucial role in the observed blackbody radiation spectrum and intensity.

We now focus on the second reservoir, which is associated with deformations of the distribution of charge of the individual vortons themselves. The possibility of such deformations leads to a polarizability of the vorton charge and hence to a polarizability of the BL itself. There are two types of polarization to consider: 1) a spatial shift in the local charge density (a perturbation displacing δq of the distribution q) and 2) a perturbation in a

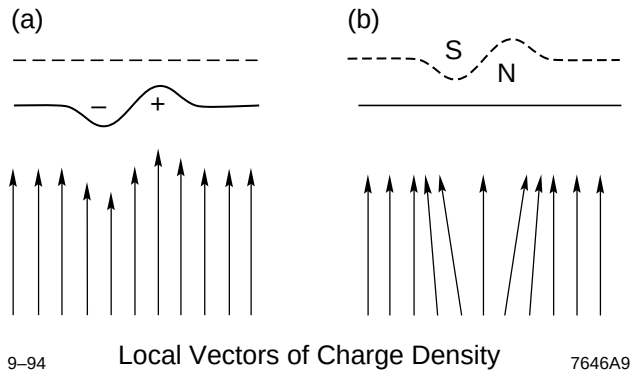

Figure 11. The spatial distribution of electromagnetic charge of the vorton is depicted here as a sequence of (adjacent) local vectors of charge density. $\bar{\Theta} = \pi/2$ (*i.e.*, positive electric charge) is assumed. Pertubations in the charge distribution that would result in vorton polarization are indicated by a systematic variation in these local charge vectors. The relative magnitude of the local magnetic charge is indicated by the dashed line, that of the local electric charge by the solid line.

a. Perturbation in the local charge magnitude will result in an electric dipole, as indicated.

b. Perturbation in the local dyality angle will result in a magnet dipole, as indicated.

local dyality angle by $\delta\Theta$ away from the (mean) value $\bar{\Theta}$. These perturbations are depicted in Fig. 11. It can be seen that perturbations involving δq lead to the usual type of polarizability (electric charge polarized by electric fields, or the analogue of magnetic charge polarized by magnetic fields) while those involving $\delta\Theta$ will lead to a new type of polarizability: electric charge magnetically polarized by magnetic fields, or its analogue, magnetic charge electrically polarized by electric fields. Full dyality symmetry is maintained.

To assist us in understanding this mechanism we again turn to known physics. In a solid, the polarization per unit volume[52]

$$P = \sum_i E^i_{loc} N_i \alpha_i, \tag{21}$$

where E^i_{loc} is the local field at the i^{th} atom, N_i is the number of atoms of type i per unit volume and α_i is the polarizability of an atom of type i. This polarizability leads to the (relative) dielectric constant

$$\epsilon = \frac{1 + \frac{8\pi}{3} \sum_i N_i \alpha_i}{1 - \frac{4\pi}{3} \sum_i N_i \alpha_i}. \tag{22}$$

For a BL, which has a continuous charge distribution, we can replace $\sum_i N_i \alpha_i$ with $\mathcal{A}$, yielding as an analogue to Eq. (22):

$$\epsilon = \frac{1 + \frac{8\pi}{3} \mathcal{A}}{1 - \frac{4\pi}{3} \mathcal{A}}, \tag{23}$$

where $\mathcal{A}$ is the polarizability per unit volume, a parameter deriving from the intrinsic vorton polarizability, but augmented by the number density of vortons in the BL. We would expect to have a similar equation for the second type of polarizability with the $\mathcal{A}$ replaced by an analogue quantity $\mathcal{B}$.

It is important to observe that since the vorton charge distribution is smooth and continuous, we would expect that once we are at wavelengths $< \bar{a}$, $\mathcal{A}$ and $\mathcal{B}$ would remain relatively flat up to very high frequency. This transition at $\bar{a}$ is similar to those in solids where there are relevant structural features of the material in question and the physics of polarizability changes with wavelength accordingly. (*cf.* Ref. 52, Fig. 7.6). In the case of BL, however, there is only one such structural feature, which is characterized by the dimension $\bar{a}$, and hence only one such transition.

The important result that Eq. (23) offers us is that if $\mathcal{A}$ or $\mathcal{B} > 0$ (we also assume that $\mathcal{A}$ and $\mathcal{B} < (3/4\pi)$, averting a polarization catastrophe),[52] which is what one would expect, then $\epsilon > 1$. And furthermore, we can expect $\epsilon > 1$ to extend up to very high frequencies—much higher than any that are relevant to our region of interest here.

If one now assumes that the (generalized) permeability of the vorton is negligible ($\mu = 1$), then the index of refraction

$$n = \epsilon^{1/2}, \tag{24}$$

and the velocity of light in the medium

$$v_\gamma = c/n = c/\epsilon^{1/2} < c. \tag{25}$$

Eq. (25), of course, enables Čerenkov radiation into a medium by a charged particle with a velocity $v_p > v_\gamma$. Čerenkov radiation, then, is the mechanism proposed for core heating.

To estimate the energy transfer from a fast charged particle to the core as an electromagnetic medium, we can use the equation for energy loss per unit path length by Čerenkov radiation: [53]

$$\frac{dI(\omega)}{dx} = \frac{e^2\omega}{c^2}\left[1 - \frac{v_\gamma^2}{v_p^2}\right], \tag{26}$$

the condition for radiation being

$$v_p > v_\gamma; \tag{27}$$

ω is the (angular) frequency of the gamma radiation.

The energy loss per unit path length, then, is

$$\frac{dI}{dx} = \frac{e^2}{c^2}\int \omega\left[1 - \frac{v_\gamma^2}{v_p^2}\right]d\omega, \tag{28}$$

where the integral is over the range of ω for which Eq. (27) is satisfied. Assuming that the bracket is a slowly varying function, Eq. (28) becomes

$$\frac{dI}{dx} = \frac{e^2}{2c^2}\left[\omega_{max}^2 - \omega_{min}^2\right] < 1 - \frac{v_\gamma^2}{v_p^2} >, \tag{29}$$

where the bracket <> indicates a suitable average over the range of integration. Eq. (27) ensures that <> is positive. Since there is no small scale structure to the vorton, ω_{max} can range up to the full energy of the particle (divided by $\hbar$); ω_{min} can be set to zero without introducing serious error. This result shows that energy loss by Čerenkov radiation will rapidly bring the particle down to the velocity v_γ, at which point the Čerenkov radiation ceases. This is essentially a classical result; this energy enters the core charge as a classical photon-like "shock wave."

From Table D-I in Appendix D, it can be seen that decay muons and pions can be expected to be relativistic, while decay positrons will be ultra-relativistic. Thus, positrons

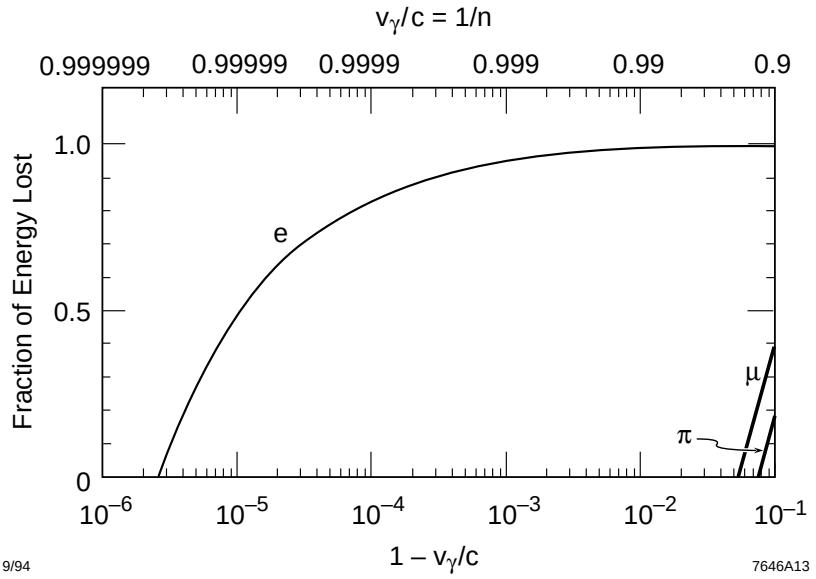

Figure 12. Relativistic energy loss by Čerenkov radiation as a function of the index of refraction $n = c/v_\gamma$ that characterizes the BL core. The particles (e, μ, and π) are all assumed to start with a kinetic energy of 220 MeV. The Čerenkov threshold (for 220 MeV) is the point at which the curves abruptly rise from the (Loss = 0) line at the bottom of the figure.

would be much more effective as Čerenkov core heaters. Specifically, for positrons (assuming a kinetic energy of 220 MeV) the Čerenkov threshold is at n = 1.00000268. For muons and pions (having the same kinetic energy), it is at 1.057 and 1.085, respectively. In Fig. 12, the fraction of energy loss by a particle (e, μ, or π) traveling through a BL core is given as a function of the velocity of light in that core. It can be seen that there is a large range in the index of refraction for which only the positron contributes to core heating. (The muons and pions are below Čerenkov threshold.) Furthermore, throughout most of this range, the positron will give up most of its kinetic energy.

From this discussion, we see that even if there is only a minute amount of vorton polarizability, we can expect that core heating by nucleon decay (positrons) will be reasonably efficient. While at the present time there is no reliable way to estimate $\epsilon, n,$ or v_γ, the use of a "reasonable" number for v_γ is instructive. For $v_\gamma = 0.999\ c$, the Čerenkov process will

transfer essentially all of the positron energy (but no muon or pion energy) into the BL core. Using this result and a crude estimate ($\sim 3/18$) for the fraction of the energy/decay carried by the decay positrons as indicated in the set of Eq. (20′) listed in Appendix D, heating efficiency would be $\sim 15\%$. That is, ~ 150 MeV/decay would end up as core heat. (It is also conceivable that the relativistic and pions would also satisfy the Čerenkov radiation condition. To the extent that this is true, the the heating core efficiency would be higher.) About the highest efficiency one could postulate, in which the BL would extract all of the positron, muon, and pion energies, is $\sim 90\%$; the neutrinos will always escape with their kinetic energy. Thus, in rough approximation, we can say that the core heating efficiency

$$\eta_{ch} = 10^{-1\pm1}. \tag{30}$$

The next conceptual step is to enter the quantum domain and assume that the core degrees of freedom are appropriately analyzed in terms of core excitations or normal modes. It is useful to think of these core excitations as analogues to excitations in solids,[54] *e.g.*, phonons, plasmons, photons, *etc.*Through a variety of scattering processes (nonlinearities), these excitations will become thermalized,[55] and they will then be characterized by Maxwell-Boltzmann or Bose-Einstein distributions at some temperature. The details of the thermalization process are not important, as long as the process is sufficiently rapid to reach something like an equilibrium temperature. This temperature will then lead to observable blackbody radiation, discussed in the next section.

7. Blackbody Radiation

a. General Remarks

The mechanism that in this model is postulated to be the explanation (for the major part) of BL luminosity is blackbody thermal radiation from the BL charge. This process appears to be the most efficient in terms of visible photon energy per nucleon decay, and perhaps more important, given appropriate circumstances, it can exhibit features that are in reasonable accord with (the wide variety of) observations.

Possible other sources for the BL luminosity, *i.e.*, scintillation of air molecules and electrical or corona discharge, are discussed in Appendices D and E, respectively. But these sources do not appear to be satisfactory explanations for the major part of BL luminosity; they have a low energy conversion efficiency into visible photons and they would not be expected to exhibit the variety of colors that have been reported. That is, their photon emission derives from radiation transitions between states of specific energy (hence yielding a sum of specific spectral lines). And while one could argue that the emitted spectral lines could correspond to one or even a few of the observed BL colors, this process is not consistent with the wide variety of observed colors and, furthermore, emission in the form of line spectra does not easily explain observations in which the BL actually changes color.[3] In fact, it is the observation of color changes that is perhaps the strongest argument for a blackbody radiation mechanism.

b. Color Temperature

As background for this discussion, let us review common experience. We know that as one heats up a blackbody, at about 800 K one can just barely see (in a darkened room) a dull red glow. As one continues to heat the blackbody, it changes color from dull red to red to orange to yellow to white as the peak of the emitted power continues to move on to shorter wavelengths. These various (perceived) colors, then, are used to define a color temperature T_c which is (essentially) equal to the temperature of the radiating blackbody. (Optical pyrometry is based upon this principle.) When the peak of the blackbody thermal radiation spectrum is in the wavelength defined as green (490 to 560 nm),[56] the emitted spectrum is actually perceived as white light because the emission power per unit wavelength is almost flat throughout the visible region. As interesting reference points, I note that the range of equivalent blackbody temperatures that are defined as "white" for the purposes of signal lights[57] is from 3000 to 6740 K. The CIE Standard Source A corresponds to a tungsten lamp at 2854 K, and is classified as white/yellow. Standard household lamps generally run cooler than this—around 2400 K. The incandescent spot on the anode of a carbon or tungsten arc at atmospheric pressure ranges from 4000 to 4250 K.[58]

Now turning to BL data, we look at a recently tabulated frequency of observed BL colors for 4112 events[7]:

Color	Percent
White	20.9
Red, Pink	17.7
Orange	23.1
Yellow	20.2
Green	1.4
Blue, Violet	11.4
Mixture	5.3

Thus, we see that blackbody thermal radiation has color characteristics which make a good match to (most of) the observed BL colors (the exceptions being Green and possibly Mixture). While there is less data on earth lights, luminosity due to thermal radiation also appears to be a good match to observation, although green lights are reported here as well.[59] The different observed colors, then, have a T_c which would be directly related to the temperature of a blackbody radiator, where the T_c will range from 1000 K and up. It is difficult to set a maximum temperature; it would depend upon whether the luminosity of the blue BL's is strictly of thermal origin or not. The color temperature of blue sky is estimated to be $\sim 2 \times 10^4$ K,[56] which, since it significantly exceeds the other color temperatures, constitutes an empirical basis for an argument that there may be nonthermal contributions to BL luminosity as well.

Thus, it is possible to account for $\sim 90\%$, or more, of the observed BL colors with a simple model of blackbody thermal radiation. The green colored BL's, and perhaps (some of) the blue ones as well, might be better explained as due to Čerenkov radiation (anyone who has looked into the water pool surrounding a nuclear reactor will recall the characteristic green light due to Čerenkov radiation.), or perhaps to gas scintillation. As is apparent from Eq. (26), Čerenkov radiation tends to have a higher spectral intensity at shorter wavelengths. This Čerenkov radiation could be escaping gamma rays (perhaps somewhat degraded in energy) from the original heating mechanism rather than the subsequent thermal radiation. (Thus, the lack of a complete thermal equilibrium may play a role here.) Also, it is possible

that absorption processes could be at work, which could distort the originally radiated blackbody spectra. On balance, while the green and possibly blue BL raise a question, it should be kept in mind that we are only talking about $\sim 10\%$ of the observations; this fraction does not seem large enough to reject the general utility of the blackbody thermal radiation model as an explanation for BL luminosity.

There is one other important set of data which is both consistent with the blackbody radiator model for BL luminosity and difficult to explain by other models. These data are the reports of color changes.[3] While in the case of BL, only a small fraction of the observations report this phenomenon, it is so striking that serious skepticism does not seem warranted. Color changes from an initial red or yellow to a dazzling white ball would in this model be explained by an increase in the blackbody temperature of the ball. Accompanying this increase in temperature is a large increase in intensity. (The total power radiated by a blackbody obeys the Stefan-Boltzmann law[60] and is proportional to the fourth power of the absolute temperature.) However, color change from violet to white has also been reported. These data do not fit quite so well into this picture because violet has a higher color temperature than white. Thus, for these reports to fall within the scope of this BL model, either the perceived violet color might in reality be a very dull red associated with a low temperature, or perhaps it is due to an mixture from a nonthermal source, *e.g.*, Čerenkov or scintillation radiation. (One must also keep in mind that the designation of BL and earth light colors is by human observers with their attendant errors in perception.) It is appropriate to note here that there are numerous observations of color changes in earth lights, and these color and intensity changes appear to be qualitatively consistent with the hypothesis of blackbody radiation[61] and kinetic temperature.[62]

c. Optical Thickness

An optically thick, blackbody radiator has recognizable features which an alert (and knowledgeable) observer can discern: 1) when hot enough to radiate, the intensity of radiation is uniform over the surface, independent of the angle the radiating surface makes with the line of observation; and 2) when the radiator is too cold to radiate a significant amount of energy in the optical region, it will completely absorb the (optical) radiation that

falls on it, manifesting a totally black object.[63] Keeping these features in mind, it is possible to argue that we are (more likely to be) dealing with a blackbody radiator (an optically thick source) rather than a graybody radiator (an optically thin source); examples of both 1) and 2), above, have been observed. Totally absorbing objects are particularly strong evidence for the blackbody (versus graybody) model.

As an example of the hot radiator case, a scientist (known to the author) got an excellent opportunity to observe a blue-white (22 ± 2 cm dia) BL from close range (50 cm) and concluded from the distribution of intensity over the sphere that it was an optically thick object.[64] And examples of BL in the second category have also been observed.[65] Furthermore, black disks or balls have been seen in conjunction with volcanoes[61] as well as with no obvious source.[66] Thus, there is again a unity in the BL and earth light phenomena in that there exist both hot and cold BL as well as hot and cold earth lights, and this BL model is able to accommodate in a natural way observations that to date have otherwise evaded explanation.

d. Intensity

1) Problem

While modeling the core of a BL as a ball of electromagnetic charge, that when cold absorbs like an optically thick blackbody and when hot radiates like an optically thick blackbody appears to give reasonably good qualitative agreement with observed colors (including a totally absorbing black) and color changes, there is a serious problem. One cannot simply postulate enough core heating to put T_s into the range of observed T_c. A blackbody radiating a characteristic white or even yellow light would be a much more powerful source of heat and light than BL is observed to be.

A sample calculation will illustrate this problem. The total radiated power P of a blackbody[60] of temperature T and area A is

$$P = \sigma T^4 A, \tag{31}$$

where $\sigma = 5.6686 \times 10^{-12}$ W/(cm^{2}K^4) is Stefan's constant. Consider the Jennison report[64] of a BL of 22 cm diameter (spherical area $\sim$ 1500 cm^2) and of blue-white color—a typical report.

If one assumes a blackbody color temperature of 3200 K (which is in the color temperature range defined as "white"),[57] then the total radiated power from this BL (modeled by a blackbody) would be $\sim 9 \times 10^5$ W, and the power in the visible spectrum would be ~ 70 kW. And even if we argued that the color temperature should be reduced by a factor of 2 to 1600 K, putting us in the orange region, we would still be dealing with a BL emitting a total of ~ 56 kW with several kW in the visible range. This result is clearly at variance with the report, for Jennison estimated the optical output to be 5-10 W and stated, ". . . the object did not seem to radiate any heat."

Thus, we have arrived at a paradox: the character of the bulk of the observations suggests that BL and other earth lights are blackbody radiators at some appropriate temperature, but a straightforward calculation of the total radiated power by such a blackbody using the appropriate color temperature yields total intensities far too large to be in agreement with observed intensities of light or heat.

One way around this problem would be to assert that BL (and also earth lights) are optically thin. But, as discussed in the last section, this is not in accord with with cases of total blackbody absorption[61,65,66] or with the conclusion of Jennison himself. Furthermore, as we can see from the above sample calculation, to postulate an optically thin or graybody solution to the Jennison report, for example, would call for a factor of at least 10^3 reduction in emissivity and in the optical density of the BL. By the second law of thermodynamics, a reduction of emissivity, or radiating power, entails at the same time an equivalent reduction in absorptivity. If this were the case, such an object would be essentially transparent with no significant ability to absorb incident radiation. As such, it would be almost impossible to observe unless it were radiating (*i.e.*, totally unsuitable as a model for the black BL and earth lights). And even in the presence of radiation, Jennison, for example, would have been able to see right through the BL. In contrast, however, he observed that the BL had "an almost solid appearance." Hence, to find consistency, we must look for another possibility in this BL model for a satisfactory resolution of this contradiction.

2) Resolution

The possibility of a resolution is found by a closer look a the details of the BL as a blackbody radiator. Recall that in this model, it is the excitations (of polarization) of the charge of the BL vortons that are emitting the thermal radiation. But at the same time these BL vortons, when viewed as a gas, are moving with velocities consistent with their kinetic temperature[67] T_k. These motions will Doppler shift the radiated blackbody energy to a higher color temperature when they are toward the observer and shift it to a lower color temperature when they are away. Using Eqs. (3) and (4), one sees that for ground state BL vortons (and $a = 1$ cm) these velocities will be relativistic for any

$$T > \frac{5Q_0^2}{2\pi a k_B} \sim 1 \text{ K}. \tag{32}$$

Of course, collective effects will tend to increase the effective mass and hence reduce the velocity of BL vortons, but such effects will be diminished on the "surface" of the BL (lower vorton density), which is where the observed blackbody radiation would emanate from.

Specifically, the formula for the observed (Doppler shifted) frequency of a photon radiated from a object moving with a velocity $\pm\beta = \pm v/c$ (toward or away) is[68]

$$\omega' = \omega\left(\frac{1 \pm \beta}{1 \mp \beta}\right)^{1/2} \equiv B\omega. \tag{33}$$

Using Eq. (33), it is easy to show that the uniform Doppler shifting of a blackbody spectrum of temperature T by a Doppler factor B will lead to another blackbody spectral shape characterized by temperature

$$T' = BT. \tag{34}$$

After shifting, the radiated power density, however, will go like BT^4 rather than $(T')^4$. One can refine this picture yet further by recognizing that B is not a single number, but will be taken from a distribution dictated by the kinetic velocity distribution associated with T_k. Although this process will yield a sum of blackbody spectra (this might also help explain some of the observed colors and color mixtures), the spectra upshifted by the largest B factors

will be the most significant and will tend to be those that characterize the observations. This means that it will be the tails of the (kinetic) velocity distribution that are the most important. Furthermore, it will be those vortons with the largest radial momentum that will penetrate to the surface of the BL.

Denoting the effective (weighted) frequency upshifting factor by $\bar{B}$, one can write

$$T_c \sim \bar{B} T_s. \tag{35}$$

As discussed above, the weighting process to determine an appropriate $\bar{B}$ will emphasize the (low probability) tails of the T_k distribution. The color temperature of a BL, then, is derived from a blackbody spectrum upshifted (mainly) by the high velocity tails of the kinetic motion of the vortons. And since it is only the vortons in the tails of the curve that (effectively) participate (recall, of course, that the tails are sparsely populated), the total radiated power will still be determined by the temperature T_s. That is, the total power will still go like $\sim T_s^4$. Thus, this mechanism renders it possible to have a T_c appropriate for blackbody radiation into the visible spectrum and still have a relatively cool, low-power radiator; the problem is resolved.

As an example, we revisit the Jennison report. Jennison reports an optical output of 5-10 W, which we assume to mean 5 to 10 $\mathrm{W_W}$; 5 to 10 W of true optical output (*i.e.*, optical photon power) would be equivalent to a tungsten light bulb power rating of 320 to 640 W.[69] This would be an extremely bright light—not appropriate to the term "glowing sphere" used by Jennison. At 5 to 10 $\mathrm{W_W}$, or $\sim 10^{-1}$ W of actual visible photon power, the Jennison sighting is roughly 10% of the mean BL value[38] of 68 $\mathrm{W_W}$ (or ~ 1 W of photon power), which is shown below to require a radioactivity $\mathcal{R}_{BL} \sim 1800$ Ci to sustain it. (An 1800 Ci BL releases a total of 10^4 W.) Thus, the Jennison BL would have had $\mathcal{R}_{BL} \sim 180$ Ci, releasing ~ 1000 W of total power. Using $\eta_{ch} = 0.1$ means the core received a heating power[70] of ~ 100 W. Using Stefan's law, it is easy to show that a blackbody core of 1500 cm^2 area and a temperature of $T_s \sim 370$ K will be in thermal equilibrium at this power level.[71] Thus, the estimated core temperature is $\sim$ 100°C or 212°F, somewhat above ambient, but not much, and is consistent with observation, *i.e.*, no noticeable heat. Using a Doppler shift factor of

$\bar{B} = 10$ ($\beta = 0.98$), say, would yield a $T_c \sim 3700$ K, a reasonable number for the observed visible spectrum. Using the efficiencies postulated in the next section, one expects 0.1 W of optical photon power, and the blackbody mechanism of this model has the capability to give a fully consistent description for this well-reported BL observation.

8. Luminosity Components

a. Blackbody Radiation

In Appendix D, using data for pions stopping in carbon, estimates are made for the more likely secondary reactions that can be anticipated as a result of the primary nucleon decays, represented by Eq. (20), taking place inside a nucleus. As described above, it is the relativistic charged particles (e^+ and possibly μ^+ and $\pi^\pm$) that would, in this BL model, be responsible for the core heating.

For the purposes of estimating the efficiency of the blackbody process, one can use the approximate efficiency factors of the several steps from radioactive decay, which yields 5.6 W/Ci (see Appendix D), to visible photons:

$$\text{Core heating efficiency} : \eta_{ch} \sim 10^{-1}$$

$$\text{Doppler upshifting fraction} : \eta_{du} \sim 10^{-2}$$

$$\text{Visible fraction of upshifted blackbody spectrum} : \eta_{vf} \sim 10^{-1}$$

This yields an overall efficiency estimate of 10^{-4} (visible photon energy/radioactive energy released) for the blackbody process. Using the tungsten lamp efficiency of 0.0156, this corresponds to 3.6×10^{-2} W_W/Ci. Needless to say, this estimate is subject to considerable uncertainty but it, with observed BL luminosities, can be used to estimate a range for BL radioactivity $\mathcal{R}_{BL}$.

The range of observed luminosities in terms of a standard tungsten light bulb[72] is from 10 to > 200 W. A statistical fit of a sample size of 1918 BL reports to a log-normal distribution function,[38] yields a geometric mean value of 68 W_W. It is useful to convert the 68 W_W back

into actual radiated power as visible photons. Again using 0.0156 as the absolute efficiency factor, we obtain

$$68\ W_{\rm W} \rightarrow 0.0156 \times 68 \cong 1\ {\rm W_{vis}}\ , \tag{36}$$

which, using the above efficiency factors for the blackbody radiator model, corresponds to $\sim 10^4$ W of radioactive decay power. Again, using the ratio 5.6 W/Ci, one calculates that the mean observed BL luminosity of 68 $\rm W_W$ requires in this model $\mathcal{R}_{BL} \sim 1800$ Ci to sustain it. Similarly, the luminosity range of 10 to 200 $\rm W_W$ converts to a range in $\mathcal{R}_{BL}$ of 280 to 5600 Ci.

b. Scintillation Light

There is also a category of lower energy particles that evolves from the nuclear absorption of energetic pions of several hundred MeV energy. Before they emerge from the nucleus, these energetic pions tend to form Δ's, which in their subsequent decay tend to eject nucleons from the nucleus. Sometimes these nucleons will pick other nucleons as they leave the nucleus. In addition, there is simple evaporation of low energy particles from the heated nucleus. The particles from these processes (p, n, d, t, ^{3}He, α) comprise a low energy, short range component of the decay radiation. (Actually, the neutron, being neutral, would be expected to have a relatively long range – some hundreds of meters, with some fraction traveling a kilometer or more. And these also should be detectable with suitable instrumentation.) These particles, mainly those with $Z \geq 2$, would generate considerable local ionization, which would lead to a component of BL luminosity by scintillation of the local air molecules. The efficiency of this scintillation process is estimated (in Appendix D) to be 3×10^{-6} (visible photon energy/radioactive energy released) with a yield in terms of an equivalent power rating of a tungsten lamp ($\rm W_W$) of 10^{-3} $\rm W_W$/Ci. This is small ($\sim 3\%$) in comparison to the yield by the blackbody process, estimated above.

c. Corona Discharge

In Appendix E, it is estimated that the corona discharge process will yield $W_{vis} \sim 10^{-6}$ W/Ci, which is equivalent to $\sim 10^{-4}$ $\rm W_W$/Ci. This is considerably smaller

than direct scintillation light and even less relevant when compared to blackbody radiation. Hence, in this model, the corona discharge plays no significant role in BL luminosity.

d. Some General Remarks

While these estimates indicate that blackbody thermal radiation would dominate the light due to scintillation or corona discharge, it is certainly conceivable that scintillation light might be significant enough to contribute to the observed blue (or green?) in BL, and also possibly to the appearance of illuminated layers[73] around a central BL core. Čerenkov light may play a role here too.

It is, of course, straightforward to apply this BL model to other luminous phenomena, *e.g.*, the Hessdalen lights, where a luminosity diameter of a meter or more has been observed, and the luminous power may range up into the thousands of $\mathrm{W_W}$.[74] The physics of the light generation would be the same, but the requisite radioactivity for earth lights would be proportionately higher. This would result from higher values of N_v and L_d for earth lights.

9. BL Shape

Most of the observed BL are spherical, but there is a significant fraction of other shapes recorded, *e.g.*, elliptical, pear-shaped, disk, cylindrical, *etc.*[1,3,7] Looking into earth light data, we note that a variety of luminous shapes have also been reported at Hessdalen.[10] While no analysis using this model has been performed on this aspect of BL, it is worth mentioning that if the poloidal and conventional dipoles of the constituent vortons should mutually align, in a fashion analogous to ferromagnetism, say, that significant departures from the most frequently observed spherical shape could be expected.

10. BL motion

It is calculated in Appendix E that the particles ejected from the nuclei constitute a net positive radial current of $I_r = 6 \times 10^{-9}$ A/Ci. Some (most?) of the particles which comprise this decay driven current have hundreds of MeV in kinetic energy and consequently will come to a stop at a considerable distance from the BL. For the region close to the BL, it is also appropriate to include the protons in I_r, for with a range of 1.4 m, they will stop outside the

luminous region of the BL. To the extent that these particles escape from the BL core, this current leaves the core region of the BL negatively charged. This residual negative charge will induce a counter current flow I_r', which will tend to neutralize the (negative) charge. I_r' will consist of a flow of positive (negative) ions in the air toward (away from) the BL.

It is proposed that this negative residual charge at the BL and the ionic currents that it induces in the air are major factors in the motion and mobility of the BL (at least when BL velocities are rather small). For example, in many accounts BL is seen descending from the clouds. Now it is known that usually the cloud base of thunderstorms is predominantly negatively charged. In this BL model, then, the electrostatic field from the base of the cloud would push downward the negative ions generated by the primary nucleon decays induced by the BL. If the BL were entrained[75] by these downward moving (local) negative ions, then it would descend with them. This downward motion would stop at some height above the ground when the flow of negative ions (as part of I_r') away from the BL region builds up a surface charge on the ground that would be of sufficient strength to cancel out the original field from the cloud. At this point, there will be a vertical equilibrium, but the BL would still be free to move horizontally. Gentle horizontal drifting motion above the ground is often observed, as, for example, in Ref. 45.

If the BL is inside a room (as is often the case), then these radially moving negative ions will deposit on the walls (one assumes that the high energy particles from the nucleon decay will penetrate the walls and thus be too far away to influence BL motion), and if the walls are poor conductors, these negative ions will build up a static surface charge. This accumulation of negative charge on the walls will tend to repel the residual negative charge at the location of the BL. This effect would lead to the observed motion of BL parallel to the walls of a room. In addition, one can see that this effect would also account for the fact that BL often tends to avoid walls and various other solid objects – often opting to go through an open window or door. This mechanism could also account for the often seen propensity for a BL to move toward a conductor. If the conductor has a path which tends to drain off the negative charge to ground, then it, like the open window, will represent a place where there is no negative charge build-up; the negative charges on other surfaces will push the BL towards the conductor.

Rapid motion of BL and earth lights is also often observed. For example, one of the Hessdalen lights was tracked by radar at a speed of $\sim$ 8500 m/s or $\sim$ 18,000 mi/h. Whether this motion is simply a case of Newton's first law[76] in action (one can only speculate about the nature of the initial impulse) or the result of some propulsion mechanism is an intriguing question that needs further consideration.

11. Multiple BL

Occasionally, two (or more) BL are reported in a connected geometrical arrangement.[1,65] Similar examples of multiple lights in geometrical arrangement have been reported at Hessdalen.[10] It is evident that, as in Appendix B, an energy minimization can be performed on this multilight system by augmenting the number of independent parameters to include not only r_i, the radii of the individual lights, but also the distances R_{ij} between the i^{th} and j^{th} lights. When this is done, for the same reasons as with the r_i (*cf.* Appendices B and C), one expects to find energy minima (and hence points of stability) with variations of the R_{ij}. Thus, not only does the mechanism of dyality rotation give stability to the individual lights, it also can give stability to geometric configurations of two or more lights.

12. BL Decay

And now it is time to consider BL decay, for which purpose it is useful to refer to Fig. 10. The lowest line can be viewed as a "decay trajectory" for an idealized BL with $T_k = 0$. A hypothetical ($T_k = 0$) BL, when formed, would be endowed with some L_d, and thus be located somewhere on this $T_k = 0$ curve. As L_d diminishes due to dissipative forces, the locus of the BL would move along the curve to the left until it would be on the $\omega_{eq} = \omega_0$ portion. (For a smaller initial value of L_d, it might even start on this portion). With further dissipation of L_d, the locus would continue to move to the left, maintaining $\omega_{eq} = \omega_0$, until $L_d = 0$. In principle, a BL with $T_k = 0$ would be stable at $L_d = 0$, but, by Eq. (B-10), r_{BL} would be infinitely large.

This idealized picture is easily extended to include the effects of a nonzero T_k. This more general situation is represented in Fig. 10 by the family of $T_k > 0$ curves, where T_k is a parameter. Strictly speaking, when these curves are viewed as possible BL decay trajectories

for physical BL, they would not necessarily be curves of constant T_k; it is known that BL and other luminous atmospheric phenomena can vary in brightness as they evolve in time. But to the extent that T_k doesn't change as the BL evolves in time, the decay trajectory of a BL or earth light will move to the left along one of these curves. Finally, as L_d continues to diminish due to dissipative forces, a threshold will be reached below which the attractive forces due to the dyality rotation are not strong enough to hold the BL together. This threshold is at (or near) the entrance to the unstable region: Coulomb repulsion and the kinetic plasma pressure take over and the vorton plasma disintegrates, dispersing the vortons.

It is possible to envisage scenarios which would be consistent with the two common modes of observed BL demise: 1) silent demise associated with a decrease in brightness and diameter, and 2) explosive demise, sometimes preceded by an increase in brightness and a change in color. It is logical that which mode a BL chose for demise would depend upon one or more of the BL parameters as L_d approached the threshold for demise. In addition, it can be seen that there is a possible feedback mechanism which would augment the instability as L_d approaches this threshold. For example, if the decay trajectory BL in parameter space ($cf.$ Fig. 10) entailed a reduction in ω_{eq}, then core heating would diminish and the core would cool and contract. This contraction would increase the Coulomb energy, increase I_d, and hence reduce ω_{eq} yet further ($L_d = \omega I_d$ is conserved), augmenting the original reduction in ω_{eq}. This would lead to the silent demise. On the other hand, if the decay trajectory in parameter space lead to an increase in ω_{eq}, then core heating would increase, expanding the core. This would cause a reduction of both the Coulomb energy and I_d. In this case, ω_{eq} would increase and again we have positive feedback. The expected sequence in this case would be further heating and ultimately the possibility of an explosive demise. It is conjectured that these two scenarios would be differentiated by T_k, as indicated in Fig. 10.

It is of interest to mention here an account[76] of E. C. Hendricks describing his observation of some earth lights at Marfa, Texas: "Prior to the moment that I observed an individual light to divide into a pair, in each case I recall, the original light grew very brilliant. I began to anticipate seeing a light divide when I noticed this quick brightening, and it usually did so." While earth light division rather than demise is the case here, I suggest that the physics is much the same as that in the explosive BL demise, just described.

III. RECAPITULATION

At this point, it is useful to summarize the above discussions by reviewing the salient features of BL as described by this model. The core, and driving engine, of BL is a coherent plasma of a large number of vortons. These vortons are scaled to the size of the lightning channel that created them, and have a size of ~ 1 cm. Not knowing the source of the vortons which comprise earth lights (*e.g.*, Hessdalen lights), no scale is assigned. (It is conceivable that the vortons in earth lights might be relics of lightning produced vortons.)

The coherent dyality rotation of these vortons, acting much like a mechanical flywheel, not only furnishes coherence forces for the BL, but also catalyzes local nucleon decay. High energy particles (mainly positrons) from this nucleon decay transfer by Čerenkov radiation a large fraction of their energy into the degrees of freedom of the BL core, heating the core to a modest temperature, 320 to 400 K, say. The heated core, acting like a blackbody radiator, radiates this energy in a Planck blackbody distribution. The relativistic motion of the individual vortons (also a manifestation of core heat) causes a Doppler shifting of the frequency of (some of) this blackbody radiation up to Planck distributions with visible color temperatures (red, orange, yellow, white, and perhaps blue) in accord with (most of the) observations. It is this Doppler upshifting which enables consistency between the observed color temperature of BL (T_c of several thousand K) and observed heat and light output of BL (very limited). The sometimes reported black BL and earth "lights" would be a coherent core, but one too cool to radiate in the visible range—even with Doppler upshifting. As a blackbody, it would absorb all visible radiation and manifest itself as a totally black object. The extensive range in size, luminosity, and lifetime of the BL and earth lights phenomena, then, can easily be accommodated by the mechanisms of this BL model. Earth lights would be governed by the same physical principles, but would be comprised of more vortons.

The catalyzed nucleon decays will drive a radial current I_r, which will build up a large electrostatic potential ($10^{5\pm1}$ V, say) at the BL location, and also cause the deposition of electrostatic charges on various surfaces in the vicinity. It is the interaction of electrostatic fields (from these surface charges and elsewhere) with the local ions that dictates the motion

of the BL, causing it to hover, drift, or move erratically. This mechanism would also account for the predilection of BL to pass through open doors and windows.

It is suggested that various BL and earth light shapes, in addition to the most common spherical shape, would be made possible by a ferromagnetic-like interaction of the dipole forces of the individual vortons.

The stability mechanism for individual BL or earth lights also applies to geometric patterns of multiple BL or earth lights. This fact, then, furnishes an explanation for such sightings. (One such sighting of three lights in a row was made here at Hessdalen as recently as last Sunday, before the start of this workshop.)

The lifetime and decay mode of the BL will be governed by a trajectory in BL parameter space as the angular momentum L_d of the dyality flywheel dissipates. BL's with a large initial L_d would have a relatively long lifetime. Depending upon the specific BL trajectory in parameter space, the demise of the BL can be either silent or explosive. It is suggested that the division of earth lights, which is sometimes observed, is governed by these same dynamic principles.

Compiled data gives typical (mean of a log-normal distribution) BL parameters as follows:[38]

Parameter	Value
Diameter	19 cm
Lifetime	7.9 s
Luminosity	68 W_W
Distance away	3.5 m
Velocity	0.9 m/s
Internal Energy$^+$	2.5 to 3.6 kJ
Electromagnetic charge*	7×10^{-7} C
Radioactivity*	1800 Ci
Total Power*	10^4 W

$^+$ This estimate derives from BL effects rather than proper measurements; hence, it is not particularly useful for comparison to this model.

$*$ The last three parameters derive from this model.

IV. ASSESSMENT

At this juncture, having stepped through BL in this model from birth to death, it is appropriate to make an assessment, confronting the above detailed description with Uman's criteria.

1) Constant size, brightness, and shape of the BL for periods up to several seconds.

A mechanism (dyality rotation of the intrinsic electromagnetic charge) that holds the ball together is an integral part of this BL model. The energy and momentum stored in this dyality flywheel is central to this mechanism, giving the BL its longevity. In addition, it would operate to maintain the size of the ball over its (luminous) lifetime. At the same time, this mechanism catalyzes the release of the energy that results in the luminosity of the BL. Since dissipation of dyality angular momentum can be expected to be a slow process (dyality rotation does not furnish the BL luminosity directly, but rather through a catalysis process), the energy release rate can be expected to be relatively constant while the ω exceeds $\bar{\omega}_0$. When ω reaches $\bar{\omega}_0$, the nuclear decay reactions and hence the luminosity effectively cease. Given a sufficiently large initial impulse of dyality torque, this model easily extends to comprehend the durations of long-lived BL, and even can include the lifetimes of one hour or more exhibited by the luminous phenomena observed here at Hessdalen.

2) The considerable mobility of the BL.

Once formed, the BL of this model does not depend upon any external power source. Hence, it has no need to attach itself to anything for sustenance—as does St. Elmo's fire. The BL motion will be dictated by the electrostatic forces deriving from the charge imbalance and radial currents resulting from proton decay. Since the BL is a coherent but detached entity, it does not need to follow the motion of the local air (wind). One anticipates that electrostatic forces could easily dominate aeolian forces. BL's that do not move along with the local wind are frequently reported. The observations of BL outside of a flying aircraft, but moving along with it, are even more relevant.[1]

3) That BL doesn't tend to rise.

While it is true that the BL will deposit energy locally in the air, which will raise its temperature somewhat, the neutral component of this heated air is not "attached" to the BL. Hence the slightly warmer air would rise unnoticed, as dictated by its buoyancy, without affecting the motion of the BL phenomenon, which motion is dictated by electrostatic forces, as described above.

4) That BL can enter houses and other structures and can exist within these structures.

The BL of this model, being an independent entity, will, as described above, go where the various electrostatic forces move it. The decay driven currents and surface charge depositions make open windows and doors a favored means of entry and exit. This argument can even be extended to smaller openings such as keyholes. Being of a very tenuous nature, with little mass and no strong local interaction forces with matter, the BL of this model can penetrate (nonconducting) material objects such as glass windows with relative ease. The amount of damage it would leave depends upon the speed of penetration and the density of the material; this could vary widely.[78] Having a local energy source, BL existence inside a structure presents no problem.

5) That BL can exist within closed metal structures.

This criterion militates against BL models that draw their energy from some external electric or electromagnetic source. The Jennison report,[64] in which a BL was observed inside a modern aircraft, is typical as a basis for this criterion. Since the source of energy for the BL of this model is local (nuclear), this criterion poses no difficulty.

V. PREDICTIONS

Looking over this analysis, one can see that several unique predictions deriving from the model are possible. Most of these predictions derive from the fact that in this model the source of BL energy is nuclear, *i.e.*, catalyzed radioactivity.

The first and, perhaps the easiest to observe (although still not so easy—one has to have one's instrumentation within some hundreds of meters of the active BL or earth light) is that there should be numerous e^+e^- annihilations, resulting mainly from the annihilation of the positron emitted from the original proton decay. (There would also be contributions from the $\pi^+\mu^+e^+$ decay chain and possibly from gamma induced showers as well.) When numerous such annihilations take place at rest, a characteristic 511 keV gamma line will be seen. A rough estimate of the detection range of this signature can be obtained by noting that the radiation length for air at STP is $\sim$ 300 m. Since the total cross section for a 511 keV gamma ray in air is about twice that at higher energies (which the radiation length represents), the appropriate range for a 511 keV gamma in air at STP would be $\sim$ 150 m. The e^+ range prior to annihilation will increase the detection range of this signature.[79] If the source is copious enough, one could expect to detect this signature out to several times 150 m—possibly even to a kilometer for strong sources.

A second prediction is that the neutrons evaporating from the heated nuclei should be detectable—perhaps as far away as a kilometer or more. (Neutron cross sections are about half that of the 511 keV γ ray, hence the greater range of possible detection.)

A third prediction is that there should be a copious amount of ionizing radiation in near proximity to the BL. (To observe this effect, one should probably be within $\sim$ 10 m, or less.)

A fourth prediction is that there should be some residual radioactivity from BL, in particular in those cases in which the BL had extended contact with solid materials. A good possibility for such radioactivity would be the 511 keV and 1275 keV gammas emanating from ^{22}Na (half-life = 2.6 y) created from ^{28}Si in glass or rock with which BL had come in contact. A rough estimate (in Appendix F) for a typical BL penetrating a window

pane (in 0.1 s) yields a residual ^{22}Na radioactivity of ~ 3 μCi in the glass. A radioactivity of this magnitude should be detectable for a number of half-lives.

Fifth, since most of the long range particles will be positive (the nucleus is positive), one expects the region of the ball to become negatively charged. In Appendix E, the radial current I_r due to this effect for a BL is estimated to be 6×10^{-9} A/Ci. A "typical" BL, characterized by an estimated $\mathcal{R}_{BL} \sim 1800$ Ci, thus would have $I_r = 10^{-5}$ A. While this current would tend be neutralized by a radial flow of ions through the air, there would be a remaining equilibrium electrostatic voltage. However, even though this voltage might be as high as 10^6 volts or more, such a voltage would be difficult to reliably detect during thunderstorm conditions—although it is certainly large enough to administer a serious electrical shock.

Sixth, as with any electrical gas discharge, one might realistically expect avalanching and other unstable variations in ionization due to I_r to lead to electromagnetic interference detectable on radios and TV's. It is also possible that vibrational modes of the BL charge as a whole might be excited, (like the giant dipole resonance in nuclei)[80] leading to strong radio frequency emissions of quasi-line spectra.

A seventh prediction is that due to the dyality rotation, there should be low frequency oscillating electric and magnetic fields associated with BL. The frequency of this oscillation would be expected to be a few Hertz. While it would be almost impossible to convincingly observe such an oscillating electric field in a thunderstorm, it is conceivable that one could detect a rather small oscillating magnetic field. Using $Q_{TOT} \sim 2 \times 10^3$ esu for the charge of a (typical) BL and a minimum detectable oscillation of 10^{-5} G, peak-to-peak, puts the maximum detection range of this feature of BL at 150 m. (For every order of magnitude increase in Q_{TOT} the r^{-2} law dictates a factor of ~ 3 increase in the detectable range of this oscillating magnetic field.)

Eighth, one would expect the BL to be a strong radar target, with a radar cross section on the order of its visible size. Furthermore, there should be a transition between a strongly reflecting target to an almost completely absorbing target in the vicinity of $\lambda = \bar{a} \sim 1$ cm. Although this model's prediction of a transition wavelength is new, in view of the very well

documented data from the Hessdalen Project, the expectation of a strong radar target might be better termed a retrodiction.

VI. POSSIBLE SUPPORTIVE EVIDENCE

As mentioned earlier, there are already some BL reports that may bear on several of the above predictions. Also, many of the observations here at Hessdalen can be construed as supportive of this BL model.

It has been reported[81] that several intense bursts of gamma ray activity have been observed, compatible with the 511 keV annihilation peak, with durations of the order of a few seconds, the typical BL lifetime. There is evidence, although not conclusive, that (some of) this activity is associated with thunderstorms. Since this model is also applicable to earth lights, it is possible that some of the Ashby and Whitehead events were not BL but rather due to some form of earth light. Of course, to be considered as a proper substantiation of this model, the 511 keV annihilation data needs to be sufficiently detailed to eliminate possible competing theories of e^+ production.[82]

It has been reported[83] that in lighting triggered events, there are (multiple) prompt excess neutrons (*i.e.*, ≥ 2). This rate of excess neutrons (2.9%) is (statistically) considerably above the neutron background rate (1.2%) associated with random triggers. Thus, if one supposes that these neutrons are due to the BL mechanism described in this paper, one obtains both a substantiation of this model, and at the same time an estimate BL production rate of $\gtrsim 1.7\%$ per lighting discharge. (Note that if the lighting trigger range exceeds the neutron range, the actual rate will be $> 1.7\%$, while if the neutron range is equal to or greater than the lighting trigger range, then the value 1.7% is the proper estimate.)

Another paper[45] reports a measured radiation level in a gamma scintillation radiometer. It is not clear what this level is, however. In the original Russian version, the level is given as 1.2 millirad/h at a distance of 2 m from the BL, whereas in the English translation of that article, it is given as 1.2 Megarad/h at 2 m. (Something was gained in translation?) While this latter value is too large to be credible, it still seems to me to be reasonable to

view this data as indicative that BL manifests radioactivity at some level. There is also an old report which can be interpreted that BL can induce radiation sickness.[84] It is clear that these suggestive reports need to be confirmed with proper instrumentation before one can feel assured that the predicted types of radioactivity are indeed present. (There also exist reports that indicate that BL is not a strong source of radioactivity,[85] but again, the best test is through the use of proper instrumentation.)

It is of interest to examine in the context of this model the "water tub" account.[86] As reported in this account, the BL entered a tub of water, causing the water to boil; the heat released in this incident has been estimated to be 3×10^6 J. Now in this BL model, one expects that the nucleon decay rate triggered by the BL will be proportional to the density of nucleons at the location of the BL. Hence, since water is ~ 800 times as dense as air, it is straightforward to estimate that when immersed in water our nominal 1800 Ci BL will release energy at a rate of ~ 8 MW. Due to the higher density of water, a good fraction of the released energy will be deposited locally in the water, heating it. For the sake of argument, let us take the heating efficiency to be twice that for a BL in air, or $\sim 20\%$. Thus, the 8 MW of total available BL power yields a heating power of 1.6 MW. At this rate, it would take about 2 s for a typical BL to deposit the estimated 3×10^6 J in the water tub. (A smaller BL would take somewhat longer. Thus, this estimate has enough leeway to take into account some possible unspecified BL quenching effects in water (or maybe the BL in this instance was smaller than "typical"). This estimate shows that this BL model offers a consistent explanation for this particularly intriguing account. There are also other instances of BL heating effects—for example, a gold ring and polyester material,[87] asphalt,[88] window glass,[78] etc. The same calculation as that done in the water tub incident would apply; the amount of heating is proportional to the nuclear density of the material and the time duration of contact with the BL. Thus, the contradiction is resolved: if in intimate contact with a dense material, BL can generate very large amounts of heat and yet in air it can appear to be intrinsically a relatively cool object.

There are reports in which observers received an electric shock from contact with a BL.[89] The circumstances of these reports appear to preclude the conclusion that the shock derived from a conventional (linear) lighting stroke. It is clear that the decay driven currents can

be expected build up electrostatic potentials, and that these potentials would be adequate to deliver an electric shock upon contact.

As to electromagnetic effects, it is appropriate to mention again the event of Dmitriev.[45] He noticed an ongoing static on a small radio while the BL was in the vicinity. Similarly, during some of the Hessdalen events, a certain amount of television interference was observed.[74]

The motion of the compass "after" the event is interpreted in this model as being due to the coherent, but nonluminous, stage of BL, for which $\omega_{eq} \sim \omega_0$. In the context of this model, both of these cases, and in particular the latter, indicate that ω_0 is a fairly low frequency; if ω_0 were more than a few Hertz, the inertia of the compasses would preclude such a response. Present day experimental limits[29] indicate that $\omega_0 \gtrsim 1\ s^{-1}$, which is consistent with these compass observations. Of course, as with the reports of ionizing radiation, these reports of magnetic effects must be viewed with caution, as there are other BL reports that tend to refute them.

With reference to the above estimate of ω_0, it is relevant to note the account of Dmitriev *et al.*,[90] in which a BL was observed to pulsate in size and luminosity with an estimated frequency of 3–5 Hz. In this model, this would be a consequence of the ω ($> \bar{\omega}_0$) associated with the luminous stage. In this regard, it is important to point out that there is a photograph of a luminous object taken in 1984 here in Hessdalen[10] in which the track of the luminous object was observed to oscillate with a frequency of 7 ± 2 Hz, consistent with the BL model of this paper. Fig. 13 reproduces this photograph. One possibility to explain these oscillations in the context of this model would be to assume that this luminous object entered a region of high electrostatic field, with which the varying electromagnetic charge (due to dyality rotation at the frequency ω_{eq}) of the "BL" was interacting. Another more complicated possibility would be to assume that this earth light was suffering from some kind of dynamic instability driven at the rate of ω_{eq}, or one of its harmonics. Since the light was observed to extinguish in the course of these oscillations, one is tempted to speculate that electrodynamic tidal forces (valid for both these suppositions) caused its abrupt demise.

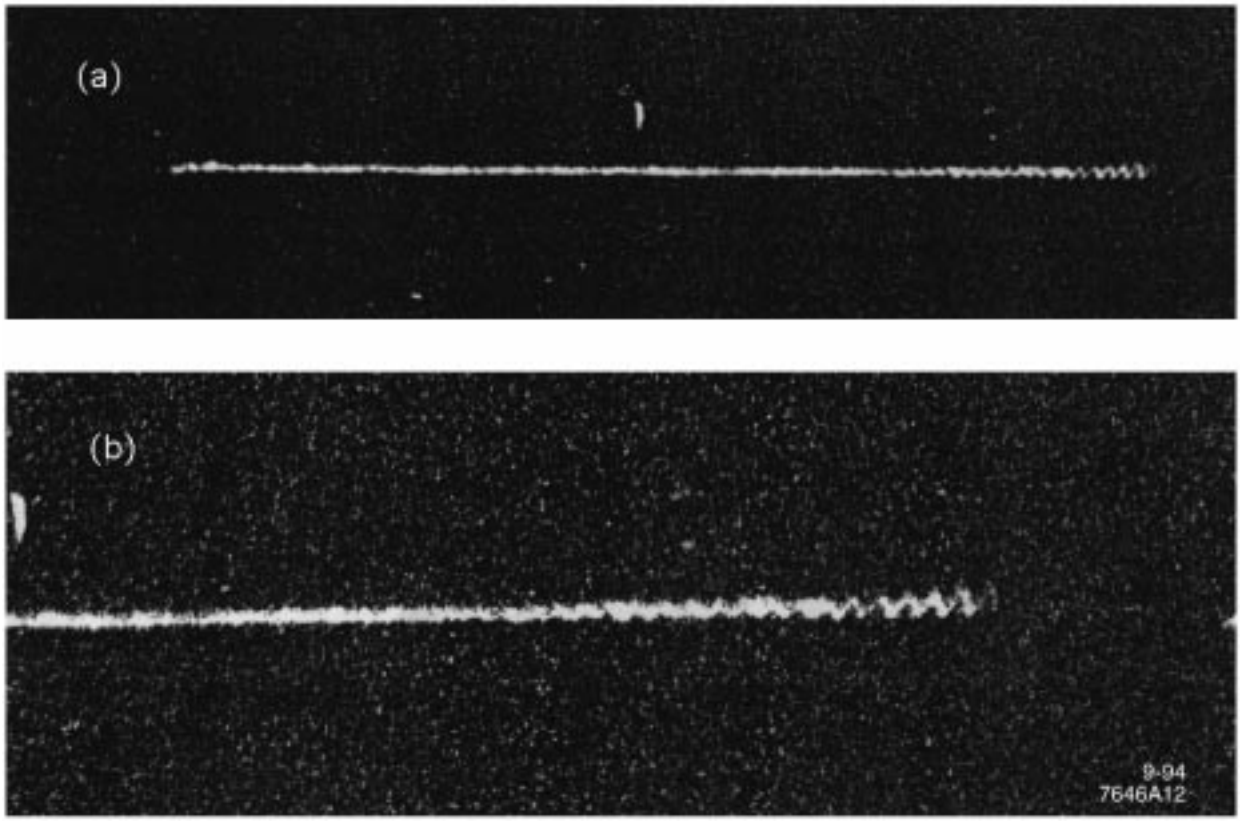

Figure 13. Photo taken during Hessdalen project (Fig. A12).[10] Reproduced with permission. The light is moving to the right. After the shutter closed, observers at the scene noted that the magnitude of the oscillation became much larger, and then the light abruptly disappeared.

a. The total exposure time (open time of the shutter) is 10 s.

b. Blowup of the last half of the path length.

As support for the prediction of a strong radar target, it should be mentioned that during February of 1984, the Project Hessdalen[10] observers reported numerous radar reflections from the luminous phenomena—often simultaneously with reliable visual sightings and/or photographs. The target return strength was on occasion comparable to that of major land targets. A radar calibration would indeed be most useful for any follow-on project. The radar cross section could then be measured and compared with other data.

VII. CONCLUSIONS

In this talk, I have described in some detail a model for BL based upon the vorton model for elementary particles. This model is able to satisfy the criteria set forth by Uman. Furthermore, when one investigates the BL phenomenon at greater depth, this model appears to be robust enough to offer possible explanations for BL size, shape, structure, lifetime, decay mode, motion, color, color changes, heat, brightness, and (stable) multiple BL geometries. In addition, many (if not most) aspects of the earth lights, such a those seen here at Hessdalen, also appear to fall within the purlieu of this model.

Finally, the analysis of this model enables a number of predictions, which were listed above. The possibility of prediction stem from the (proposed) electromagnetic nature of BL and earth lights and the fact that their source of energy stems from catalyzed nucleon decay. Suffice it to say that in appropriate circumstances these predictions should provide a definite test of this model, and I recommend that any follow-on to Project Hessdalen should incorporate appropriate instrumentation to try to verify these predictions.

ACKNOWLEDGEMENTS

Conversations with many colleagues have proven useful in the evolution of this model. In particular, I would like to thank M. Sullivan for discussions about vorton structure and physics; R. Arnold and H. Jackson for discussions about nuclear physics; E. Hoyt for information about optical pyrometry; S. Rokni for useful information about radiometry; I. Wieder for providing some useful references; E. Strand, L. Havik, and O. G. Røed for discussions about the phenomena at Hessdalen; and P. Devereux and E. Bach for interesting information about earth lights seen throughout the world. And finally, I wish to thank Erling Strand, his colleagues, and the citizens of Hessdalen for their hospitality and dedication in putting together this most excellent workshop.

APPENDIX A

Dyality Rotation of a Single Vorton

The concept of dyality rotation as a degree of freedom naturally entails an associated angular momentum L_d and energy E_d. As guidance for the understanding of L_d and E_d, we can turn to the classical equations for angular momentum and write

$$L_{d_i} = \omega_i I_{d_i} \ , \tag{A-1}$$

and

$$E_{d_i} = \frac{\omega_i^2 I_{d_i}}{2} = \frac{L_{d_i}^2}{2I_{d_i}} \ , \tag{A-2}$$

where the subscript i indicates an individual or i^{th} vorton. The quantity I_{d_i}, then, is a moment of inertia characteristic of the dyality rotation of a vorton, and $\omega_i = (d\Theta_i/dt)$ is the angular velocity of that rotation.

For insight into the nature of the quantity I_{d_i}, we note that in mechanics

$$I = \int \rho^2 dM \ , \tag{A-3}$$

which for a point mass M yields

$$I = \rho^2 M \ , \tag{A-4}$$

where ρ is the distance from M to the axis of rotation. By analogy, for the case of dyality rotation, the equivalent of the mechanical mass should be proportional to the Coulomb energy E_{c_i} which is the energy associated with the electromagnetic charge of the vorton; after all, it is the charge that is doing the "rotating." Using the Einstein relationship,[91] then, we write

$$M_{d_i} = E_{c_i}/c^2 \ . \tag{A-5}$$

In looking for the appropriate radius to associate with dyality rotation, we recall that this effect (apparently) violates the conservation of charge, both electric and magnetic.

Now, since charge violation must be associated with a range on the order of the photon Compton wavelength, it is reasonable to assume that the (effective) Compton wavelength of the photon $\lambda\!\!\!^{-}_{\gamma}$ is the appropriate length scale (What other scale is there?) and write the dyality analogue of Eq. (A-3) as

$$I_{d_i} = k_I^2 \lambda\!\!\!^{-2}_{\gamma} E_{c_i}/c^2 \ , \tag{A-6}$$

where k_I is a constant of order unity, which is included to account for ignorance about this aspect of vorton physics, *e.g.*, the extent of relativistic corrections, *etc.* [It is tempting to set $k_I = \sqrt{2}$, which would eliminate numerical constant from Eqs. (A-11) and (B-9), but such a step is better based upon empirical evidence rather than theoretical prejudice.] It is appropriate to remark here that the moment of inertia will vary with dyality angle if $\lambda\!\!\!^{-}_{\gamma_e}$, the Compton wavelength of the electric photon, and $\lambda\!\!\!^{-}_{\gamma_m}$, that of the magnetic photon, differ. But if they are roughly equal, without serious error one may define

$$\lambda\!\!\!^{-2}_{\gamma} \equiv \frac{1}{2}(\lambda\!\!\!^{-2}_{\gamma_e} + \lambda\!\!\!^{-2}_{\gamma_m}) \ , \tag{A-7}$$

and then use Eqs. (A-1) and (A-6), to obtain

$$L_{d_i} = \omega_i k_I^2 \lambda\!\!\!^{-2}_{\gamma} E_{c_i}/c^2; \tag{A-8}$$

Eqs. (A-2) and (A-6) yield

$$E_{d_i} = \frac{L_{d_i}^2 c^2}{2k_I^2 \lambda\!\!\!^{-2}_{\gamma} E_{c_i}} \ , \tag{A-9}$$

and

$$\omega_i^2 = \frac{2E_{d_i}}{I_{d_i}} = \frac{2E_{d_i}c^2}{k_I^2 \lambda\!\!\!^{-2}_{\gamma} E_{c_i}} \ , \tag{A-10}$$

or

$$\omega_i = \frac{\sqrt{2}c}{k_I \lambda\!\!\!^{-}_{\gamma}} \sqrt{\frac{E_{d_i}}{E_{c_i}}} \ . \tag{A-11}$$

APPENDIX B

BL Coherence Forces

To extend the analysis for a single vorton (in Appendix A) to a collection of vortons, one merely writes $L_d, E_d,$ and I_d, the appropriate (collective) quantities characterizing the BL, in place of $L_{d_i}, E_{d_i},$ and I_{d_i}:

$$L_d = \omega I_d \ , \tag{B-1}$$

$$E_d = (1/2)\omega^2 I_d = L_d^2/(2I_d) \ , \tag{B-2}$$

and

$$I_d = k_I^2 \overline{\lambda}_\gamma^2 E_c/c^2 \ , \tag{B-3}$$

where it is assumed that the individual vortons comprising this collection of vortons (BL) have a common angular velocity of dyality rotation ω. This assumption is justified below, where it is shown that due to dyality rotation, there are coherence forces which tend to synchronize the dyality angles of the constituent vortons. Following Eqs. (A-8) and (A-11), we write

$$L_d = \omega k_I^2 \overline{\lambda}_\gamma^2 E_c/c^2 \tag{B-4}$$

and

$$\omega = \frac{\sqrt{2}c}{k_I \overline{\lambda}_\gamma} \sqrt{\frac{E_d}{E_c}} \ . \tag{B-5}$$

Using these equations to describe the core, it is straightforward to demonstrate that there is a stable equilibrium point associated with dyality rotation. This point of stability results from energy exchange in the BL between the (static) Coulomb energy E_c and the (dynamic) dyality energy E_d. There are other components of energy in the BL, but since they enter as refinements to the basic electromechanics of BL stability, they are ignored (set to zero) in this

initial stability analysis. To proceed, then, we consider a BL of $E_{tot} = E_{tot}(E_c; L_d)$, where the functional dependance is such that E_c is (viewed as) a parameter and L_d is specified and constant. (L_d is a conserved quantity.) Using Eqs. (B-2) and (B-3), then, we write the total BL energy

$$E_{tot}(E_c; L_d) = E_c + E_d(E_c; L_d) = E_c + L_d^2 c^2/(2k_I^2 \overline{\lambda}_\gamma^2 E_c) \ . \tag{B-6}$$

We now investigate the condition $dE_{tot}/dE_c = 0$ to obtain

$$E_c = E_d = L_d c/(2k_I^2 \overline{\lambda}_\gamma^2)^{1/2} \ , \tag{B-7}$$

which, since E_{tot} is at a minimum, is a stable equilibrium point. Putting this result into Eq. (B-5) yields

$$\omega = \sqrt{2}c/(k_I \overline{\lambda}_\gamma) \equiv \omega_0 \ , \tag{B-8}$$

which is a characteristic dyality rotation frequency for a BL, independent of the number of vortons that comprise it or the angular momentum that sustains it. This result is generalized in Appendix C where it is shown that as a result of the kinetic energy in the vorton gas pressure, the actual equilibrium frequency for a BL, ω_{eq}, will be displaced above ω_0.

In similar fashion, this approach can also be used to calculate the BL radius r at the stable equilibrium point; instead of E_c as the parameter, one uses r by employing

$$E_c = \frac{Q^2}{r} \tag{B-9}$$

in Eq. (B-6) and then setting $dE_{tot}/dr = 0$. This prescription yields

$$r = \frac{\sqrt{2} k_I \overline{\lambda}_\gamma Q^2}{L_d c} \ , \tag{B-10}$$

which of course is the condition for $E_c = E_d$.

We now see the origin of internal coherence forces in this model for BL and earth lights. Looking again to a mechanical analogue for guidance, we consider briefly the rotating figure skater. Here we see that there is a centrifugal force given by $-dE_r/d\rho$, where E_r is the kinetic energy of rotation. This centrifugal force tends to extend the skater's arms, increasing the moment of inertia. The effect is to reduce the kinetic energy of rotation, putting that energy into whatever object is resisting the centrifugal force (*e.g.*, the skater's arms). Since the skater exerts no torque on any external object, angular momentum is conserved in this process.

In this model for BL, the analogous force is given by $-dE_d/d\chi_i$, where χ_i is an appropriate coordinate parameter for an individual vorton, of which there are two interesting sets. One is the distance r_i of the i^{th} vorton from the center of charge of all of the rest of the vortons, and the other is the dyality angle Θ_i of that vorton with respect to the mean (rotating) dyality angle of the rest of the vortons. As with the skater, both of these forces will tend to increase the moment of inertia of the system, reducing the energy of (dyality) rotation, while conserving angular momentum. One sees, then, that the force $-dE_d/dr_i$ will manifest itself as a force of attraction between the vortons of like charge (in opposition to the repulsive Coulomb force), tending to increase E_c and giving a spatial coherence to the BL. Similarly, the force $-dE_d/d\Theta_i$ will also tend to increase I_d and hence E_c. It does this by synchronizing the rotation of the vortons' dyality angles. The forces $-dE_d/d\chi_i$ are, of course, opposed by the forces $-dE_c/d\chi_i$. These two sets of forces are at an equality at the equilibrium point found above at which $dE_{tot}/d\chi_i = 0$.

In essence, the action of these forces transfers energy between E_d and E_c to minimize total energy. The result is an equilibrium point at which there exist attractive forces are strong enough to hold the BL core together in a state of equilibrium (once the core has been formed).

APPENDIX C

BL Equilibrium Frequency

It is of interest to explore the stability and equilibrium frequency ω_{eq} of BL when $T_k > 0$. To do this, we generalize Eq. (B-6) to include E_k, and write

$$E_{tot} = E_c + E_k + L_d^2 c^2/(2k_I^2 \overline{\lambda}_\gamma^2 E_c) \ , \tag{C-1}$$

where, as described in the text, E_k is the kinetic energy of motion of the individual vortons in a BL.

Modeling the BL core as a gas, we note that for an adiabatic process the volume V and temperature T of a gas are related by[92]

$$TV^{\gamma-1} = K_1 \ , \tag{C-2}$$

where K_1 is a constant and $\gamma = c_p/c_v$ is the ratio of specific heats. Using $V_{BL} = (4/3)\pi r^3$ and Eq. (18), we can obtain E_k as a function of r:

$$E_k = \frac{K_2}{r^{3(\gamma-1)}} \tag{C-3}$$

where

$$K_2 = \frac{N_v n_k k_B K_1}{2}\left(\frac{3}{4\pi}\right)^{\gamma-1} . \tag{C-4}$$

Thus, as a function of r,

$$E_{tot} = \frac{Q^2}{r} + \frac{K_2}{r^{3(\gamma-1)}} + L_d^2 c^2 r/(2k_I^2 \overline{\lambda}_\gamma^2 Q^2) \ . \tag{C-5}$$

Setting $dE_{tot}/dr = 0$ obtains

$$0 = -\frac{Q^2}{r^2} - \frac{3(\gamma-1)K_2}{r^{(3\gamma-2)}} + L_d^2 c^2/(2k_I^2 \overline{\lambda}_\gamma^2 Q^2) \ . \tag{C-6}$$

Eq. (C-6) can be solved for $r = r_{eq}$, but it is more useful to multiply it by r and obtain

$$0 = -E_c - 3(\gamma - 1)E_k + E_d \ , \tag{C-7}$$

or

$$E_d = E_c + 3(\gamma - 1)E_k \ . \tag{C-8}$$

Substituting Eq. (C-8) into Eq. (B-5) yields

$$\omega_{eq} = \frac{\sqrt{2}c}{k_I \overline{\lambda}_\gamma} \left(\frac{E_c + 3(\gamma - 1)E_k}{E_c} \right)^{1/2} = \omega_0 [1 + 3(\gamma - 1)E_k/E_c]^{1/2} \ . \tag{C-9}$$

For a monatomic gas[93] $\gamma = 5/3$, and Eq. (C-9) becomes

$$\omega_{eq} = \omega_0 \sqrt{1 + 2E_k/E_c} \ . \tag{C-10}$$

APPENDIX D

BL Radioactivity

Simply put, the model for BL radioactivity is catalyzed nucleon decay described by Eq. (20), where the nucleon is a member of the nucleus of an atom at the location of the BL. In Eq. (20), one of the quarks in the nucleon makes the transition, but there are two other "spectator" quarks that still are hadronic in nature; these will lead to nonbaryonic hadronic debris, *i.e.*, pions and perhaps some kaons. The number, types, and energies of the pions and kaons released in these reactions are best described by phenomenological distributions. While detailed knowledge of the π-K distributions is not essential to the concept of the BL model at this stage, the assumption that a few energetic pions would be emitted appears quite reasonable and will enable some estimates of the BL energy budget.

For the purposes of calculation, it is assumed that there are produced on the average two energetic pions (and no kaons) accompanying the lepton in each nucleon decay process, and that these three particles share equally in the available kinetic energy from the decay. (A three particle phase space would be more precise, but then one should also include the possibility of other numbers of pions and kaons as well; sufficient information is not available to justify such refinements.) Such an assumption should be good to a factor of two or three, which is quite adequate for the purposes of this appendix. In the same spirit, the following possible reactions represented by Eq. (20), assuming $n = 2$ and $m = 0$, are recorded:

$$
\begin{aligned}
vp &\rightarrow ve^{+}\pi^{+}\pi^{-} \\
vp &\rightarrow ve^{+}\pi^{\circ}\pi^{\circ} \\
vp &\rightarrow v\bar{\nu}_e\pi^{+}\pi^{\circ} \qquad (20') \\
vn &\rightarrow v\bar{\nu}_e\pi^{+}\pi^{-} \\
vn &\rightarrow v\bar{\nu}_e\pi^{\circ}\pi^{\circ} \\
vn &\rightarrow ve^{+}\pi^{\circ}\pi^{-}
\end{aligned}
$$

Final states with e^- and ν_e are precluded[15] by conservation of Q_H. Reactions to μ^+ and $\bar{\nu}_\mu$ in the final state are also possible, but their inclusion above would not substantially change the energetics (although the muons in the final state would be much less efficient at heating the BL core). For simplicity, it is assumed each reaction of Eq. (20′) has the same probability. Further, it is assumed that the leptons escape the nucleus with no energy loss and that one half of the pions also escape (without energy loss), the other half being absorbed. (Actually, since the nucleons are decaying inside the nucleus, the pion absorption rate probably exceeds 0.5, but again at this stage such a refinement is unwarranted.) Since air is 80% nitrogen, we can assume without serious error that the nucleon decays inside an ^{14}N nucleus. When a proton decays to e^+ or $\bar{\nu}_e$ we get

$$^{14}\mathrm{N} \rightarrow {}^{13}\mathrm{C} + \bar{\ell}_e + 2\pi \ , \tag{D-1}$$

where $\bar{\ell}_e$ represents the e^+ or $\bar{\nu}_e$, and the pions balance the charge. Similarly, when a neutron decays to a $\bar{\ell}_e$, we get

$$^{14}\mathrm{N} \rightarrow {}^{13}\mathrm{N} + \bar{\ell}_e + 2\pi \ . \tag{D-2}$$

For the purposes of estimation, we assume that the available kinetic energy ($\mathrm{M}_N - 2m_\pi$) $\sim$ 660 MeV is divided equally between the lepton and the two pions. Thus, we have 440 MeV escaping kinetic energy and 220 MeV + 140 MeV = 360 MeV being absorbed into the nucleus. The absorbed pion will heat the nucleus, causing a variety of particles to evaporate.

As a basis for core heating estimates, the calculations in Table D-I are useful.

TABLE D-I

Particle	Mass	Total Energy	β	$1-\beta$
$e^\pm$	0.511 MeV/c^2	220.511 MeV	0.99999732	2.68×10^{-6}
$\mu^\pm$	105.658	325.658	0.946	5.41×10^{-2}
$\pi^\pm$	139.568	359.568	0.922	7.84×10^{-2}

The calculations for Table D-I assume that the particle kinetic energy is 220 MeV. While one would realistically expect a distribution of kinetic energies, using a specific energy is useful for the purposes of comparison.

Data for the absorption of stopped π^- in carbon[94] indicates that the ejected and evaporated particles are mainly $p, d, t,$ and α. (Neutrons were not detected in this experiment.) From Table 1 of Ref. 94, we list in Table D-II the percent yields per absorbed pion and the mean kinetic energies of the distribution of particles.

TABLE D–II

Particle	Yield in %	Mean Kinetic Energy	Energy/π^-
p	39 ± 7	24 MeV	9.4 MeV
d	30 ± 5	19	5.7
t	20 ± 6	13	2.6
^{3}He	9 ± 3	47	4.2
α	81 ± 24	9	7.3
Li	1.4 ± 0.4	18	0.3

Using Table D-II, (and assuming the neutron yield equals the proton yield) the total change in atomic number is $\Delta A = -5.5$, yielding a daughter nucleus with an estimated mean atomic number of 6.5.

Based upon the above discussion (and assuming that carbon at $Z = 6$ is indicative of how nitrogen at $Z = 7$ and oxygen at $Z = 8$ will behave), we obtain the Table D-III for the estimated energy distribution among the various final state particles.

TABLE D-III

Emitted Particle	Yield per Decay	Kinetic Energy per Particle	Typical Range in air
charged lepton	0.50	220 MeV	470 m
neutrino	0.50	220	infinite
charged pion ($\pi^{\pm} \rightarrow \mu^{\pm}$)	1.0	220	1000 m
gamma($\pi^{\circ} \rightarrow 2\gamma$)	2.0	180	300 m
proton	0.4	9.4	1.4 m
neutron	0.4	9.4	500 m
deuteron	0.3	5.7	35 cm
triton	0.2	2.6	6 cm
^{3}He	0.1	4.2	$\sim$ 1 cm
alpha	0.8	7.3	4 cm
$Z > 2$	1.0	$\sim$ 20	$\sim$ 5 cm

In order to estimate the (average) kinetic energy of the daughter nucleus, we assume that 10 percent of the 220 MeV kinetic energy of the emitted pion is internally converted to kinetic energy of the final daughter nucleus. Consequently, the Z > 2 daughter (this includes the Li) will have a kinetic energy of $\sim$ 20 MeV, as is indicated in the Table D-III. (This is also consistent with the 18 MeV found for the Li kinetic energy as given in Table D-II.) Thus, $\sim$ 30 MeV/decay or $\sim$ 3% of the decay energy will be deposited locally. It is also clear from Table D-III that one expects that most of the decay energy will be transported by the high energy particles to some distance from the BL. (Note that a summation of the energy in the final state particles as tabulated above exceeds the nucleon mass by $\sim$ 4%, but for the purposes of this estimate, the implied small normalization adjustment is not useful.)

At this juncture, it is of interest to estimate the contribution of scintillation of the air to BL luminosity. If we consider, for the purposes of this estimation that Eq. (20) is proceeding at a nominal 1 Ci rate (3.7×10^{10} decays/s), then the total energy release will be $3.7 \times 10^{10} \times 0.94 = 3.5 \times 10^{10}$ GeV/s = 5.6 W (per Ci), and if there is only the usual energy

absorption mechanisms active, then $\sim 10^{18}$ eV/s or 0.17 W will be deposited locally (in the air). Based upon calculated scintillation rates for air,[95] we use an efficiency factor of 10^{-4} for the yield of this locally deposited energy (ionization and excitation) into photons in the visible region (emitted by the resulting ion pair recombinations, and emissions by excited atoms and molecules). Thus, one estimates a yield 1.7×10^{-5} W of visible photons for the nominal 1 Ci BL. It would appear reasonable to assert that this estimate is good to a factor of two or three. Using 0.0156 as the absolute efficiency factor for a typical (25 W) tungsten light bulb,[69] we find that our nominal BL of 1 Ci has a luminance equivalent to a 10^{-3} Watt tungsten light bulb. We use $\mathrm{W_W}$ as the unit for this (equivalent) quantity. Thus, the coefficient for the scintillation component of BL luminosity is 10^{-3} $\mathrm{W_W/Ci}$. The efficiency for this process (visible photon energy/radioactive energy released) is 3×10^{-6}, quite low in comparison to the blackbody thermal process discussed in the text.

APPENDIX E

BL Decay Driven Current

Due to catalyzed nucleon decay, the BL has the character of a current source, suspended in space. This current, which is due to the excess of long-range positive charges leaving the BL region, will be radial in flow pattern. Looking at Table D-III in Appendix D and setting the charged pion excess at 0.1, we estimate that on average (including both signs of pion charge), there is the equivalent of one high energy positive charge/decay. Thus, a nominal BL of 1 Ci will drive a radial current

$$I_r = 3.7 \times 10^{10} \times 1.6 \times 10^{-19} = 6 \times 10^{-9} \text{ A/Ci.} \tag{E-1}$$

As one considers larger and larger spheres out from the BL, this radial current (through the sphere) will diminish monotonically as the radius of the sphere in question exceeds the range of the high energy (positive) particles which comprise I_r.

Since the BL also creates numerous ion pairs in its vicinity, this (high energy) outward current will be balanced by radial ionic currents, positive ions flowing toward the ball and negative ones flowing away. The residual voltage that builds up at the BL to drive these currents will depend upon the ion density (and ion mobility) in the air surrounding the BL. Since ionic mobility and density is finite, there will be a voltage build up at the BL. While under these circumstances, an equilibrium static voltage at the core is difficult to calculate, it is easy to imagine that this current source can build up a (negative) static potential of 3 to 4×10^5 V, consistent with the value deduced by Dmitriev[45] from measured ozone/nitrogen dioxide ratios. A voltage of -4×10^5 V $= -1.3 \times 10^3$ statvolts for a BL of radius 10 cm implies a net ion charge $= -1.3 \times 10^4$ esu. This is comparable in magnitude to (and probably somewhat larger than) the Q_{TOT} indicated by Eq. (5). It is argued in the text that (for low velocities, at least) the motion of this negative charge dictates the motion of the BL.

If the driving I_r is large enough, this voltage may be sufficient to create additional local ionization, that is, it could generate a corona discharge. An estimate of this effect is of some interest, and, in view of the fact that the corona light is shown to be small, a crude estimate

should be adequate. Using the current of 6×10^{-9} A/Ci, and assuming Dmitriev's voltage and gradient,[96] independent of I_r, yields 3×10^{-4} W/Ci. If this power goes into photons at an efficiency of 4×10^{-3} (the corona process in air is not a very efficient way to produce visible light), then the visible photon power $W_{vis} = 1.2 \times 10^{-6}$ W/Ci the equivalent tungsten bulb power is $\sim 10^{-4}$ $\mathrm{W_W}$/Ci, an order of magnitude less than the luminance due to direct local ionization with subsequent scintillation of the air, and yet (at least) another order of magnitude below the blackbody thermal radiation from the core.

APPENDIX F

Estimate of Residual Radioactivity

One can use the estimate of the BL radioactivity in air to estimate residual radioactivity in solid materials that come into contact with a BL. I make such an estimate here for glass since it is often penetrated by ball lightning, frequently with witnesses present. While the composition of various types of glass varies considerably, the major component of most commercial glasses[97] is SiO_2. As a result of catalyzed nucleon decay, one expects the silicon and oxygen nuclei to yield daughter products of lower Z. Upon consulting the radioactive nuclides listed[60]

for A < 28 (silicon), we find:

Nuclide	Half-Life
^{3}T	12.26 y
^{10}Be	2.7×10^{6} y
^{22}Na	2.6 y

For the purposes of this calculation, the most interesting of these is ^{22}Na. This conclusion follows from the fact that the mean ΔA in the carbon data was -5.5, and the Δ A from ^{28}Si to ^{22}Na is -6. Thus, ^{22}Na would be expected to be near the peak of the distribution of the Z > 2 daughter products from BL catalized decay of ^{28}Si. In addition, ^{22}Na has a characteristic signature that would be easy to detect: two 511 keV γ's and a 1275 keV γ per ^{22}Na decay. On the other hand, ^{3}T and ^{10}Be both give off a low energy β^{-}, which would be more difficult to detect.

The reaction of interest, then, is

$$^{28}\mathrm{Si} + v \rightarrow {}^{22}\mathrm{Na} + v + \mathrm{X}, \tag{F-1}$$

where X stands for all other reaction products.

The number of BL catalyzed decays which yield ^{22}Na will be given by

$$N_c = \frac{\rho_{\mathrm{Si0_2}}}{\rho_{\mathrm{air}}} \mathcal{R}_{BL} \frac{V_{\mathrm{Si0_2}}}{V_{BL}} KT\eta_c \tag{F-2}$$

where ρ indicates density, $\mathcal{R}_{BL}$ the radioactivity of the BL in air, V denotes volume, $K = (28/60) = 0.47$ is the nucleon ratio of Si in $Si0_2$, T is the time of BL contact with the glass, and. η_c is the fraction of catalyzed ^{28}Si decays which actually yield ^{22}Na.

In order to make an estimate of N_c, we note that $(\rho_{\mathrm{Si0_2}}/\rho_{\mathrm{air}}) = (2.20/0.0012) = 1.83{\times}10^3$, assume a window pane $1/8'' = 0.3$ cm thick and use a "typical" BL with $\mathcal{R}_{BL} = 1800$ Ci. For the purpose of this calculation, the other factors for Eq. (F-2) are:

$$V_{\mathrm{SiO_2}} = \pi r_{BL}^2 \times 0.3 = \pi(9.5 \text{ cm})^2 \times 0.3 = 85 \text{ cm}^3,$$

$$V_{BL} = \frac{4}{3}\pi r_{BL}^3 = \frac{4\pi}{3}(9.5 \text{ cm})^3 = 3600 \text{ cm}^3,$$

$$T = 0.1 \ s,$$

and

$$\eta_c = 0.1,$$

which yield

$$N_c = 1.83 \times 10^3 \times 1800 \times 3.7 \times 10^{10} \times \frac{85}{3600} \times 0.47 \times 0.1 \times 0.1$$

$$= 1.3 \times 10^{13} \text{ atoms of } ^{22}\text{Na}.$$

(N.B. The 2.6 y half-life of ^{22}Na is equivalent to a 3.75 y = $1.2{\times}10^8$ s exponential lifetime.) Using the lifetime of 1.2×10^8 s for ^{28}Na, then, yields an estimated initial decay rate for the ^{22}Na left in this sample of glass:

$$\mathcal{R}(^{22}\text{Na}) = 1.3 \times 10^{13}/1.2 \times 10^8 = 10^5/\text{s} \sim 3 \ \mu\text{Ci}.$$

A radioactivity of this magnitude is not particularly hazardous and is easy to detect.

REFERENCES AND FOOTNOTES

1. S. Singer, *The Nature of Ball Lightning* (Plenum Press, New York, 1971).
2. W. N. Charman, *Phys. Rep.,* **54**, 261 (1979).
3. J. D. Barry, *Ball Lightning and Bead Lightning* (Plenum Press, New York, 1980).
4. B. M. Smirnov, *Phys. Rep.,* **152**, 177 (1987).
5. Y.–H. Ohtsuki, Ed., *Science of Ball Lightning* (World Scientific, Singapore, 1989).
6. B. M. Smirnov, *Usp. Fiz. Nauk*, **162**, 43 (1992) [*Sov. Phys. Usp.*, **35**, 650 (1992)].
7. B. M. Smirnov, *Phys. Rep.,* **224**, 151 (1993).
8. G. Egely in Ref. 5, p. 19; Y.–H. Ohtsuki and H. Ofuruton in Ref. 5, p. 31.
9. P. Devereaux, *Earth Lights Revelation* (Blanford Press, London, 1989).
10. E. Strand, *Project Hessdalen* 1984, Final Technical Report, Part One.
11. Since additional progress in the development of this model has occurred between the time of the talk in March and submission of the paper for publication in September, appropriate updates are included in this written version of the talk. The major update is a better understanding of the mechanisms leading to the heating of the BL core and the subsequent re-radiation of energy in the visible region.
12. M. A. Uman, *Jour. Atmos. and Terr. Phys.,* **30** 1245 (1968).
13. Uman's criteria militate against some of the simpler models for BL: 1) Relative stability in size and shape tends to rule out models dependent upon thermally stored energy, which would diminish in effect as the BL cooled; 2) Mobility rules out various forms of corona discharges such as St. Elmo's fire, which are attached to conductors or other material objects (such as masts or spars); 3) Not rising is another argument against a thermally driven BL; 4) and in particular 5) rule out models that rely upon external electromagnetic radiation or external electric currents as sources for BL energy.
14. D. Fryberger, *Hadronic Jour.,* **4**, 1844 (1981).

15. D. Fryberger, *Found. Phys.,* **13**, 1059 (1983).

16. O. Heaviside, *Electromagnetic Theory* (Chelsea Publishing Co., London, 1892).

17. G. Y. Rainich, *Trans. Am. Math. Soc.,* **27**, 106 (1925).

18. Y. Han and L. C. Biedenharn, *Nuovo Cimento*, **2A**, 544 (1971) introduced the word "dyality" for this symmetry to avoid the (often used, but confusing) use of "duality," which has a different meaning in other contexts.

19. N. Cabibbo and E. Ferrari, *Nuovo Cimento,* **123**, 1147 (1962); S. Shanmugadhasan, *Can. J. Phys.,* **30**, 218 (1952).

20. D. Fryberger, *Found. Phys.,* **19**, 125 (1989); *Found. Phys. Lett.,* **3**, 375 (1990).

21. A more complete discussion of the two-photon question in the context of the vorton model is planned for a later paper.

22. J. Wei and W. E. Baylis, *Found. Phys. Lett.*, **4**, 537 (1991).

23. For example, *cf.*, J. D. Bjorken and S. D. Drell, *Relativistic Quantum Mechanics* (McGraw Hill Book Co., New York, 1964), p. 64 *et seq.*; S. Saunders and H. R. Brown (Eds.), *The Philosophy of the Vacuum* (Clarendon Press, Oxford, 1991); and P. W. Milonni, *The Quantum Vacuum* (Academic Press, Inc., San Diego, 1994).

24. As an exception to this remark, one supposes that the magnetic analogue neutrinos are light, but that they couple only through the magnetic analogue of weak bosons, which do not couple to the usual (electric) particles, essentially precluding their observation. Similarly, the magnetic photon is presumed to be light, but being radiated only by magnetic charges, it also would be quite rare.

25. P. M. Morse and H. Feshbach, *Methods of Theoretical Physics* (McGraw Hill Book Co., New York, 1953), p. 666. We use here the symbols of H. Bateman, *Partial Differential Equations of Mathematical Physics* (Cambridge Univ. Press, Cambridge, 1959), p. 461, to free μ and θ for other notation.

26. Fig. 4 is adapted from R. Penrose and W. Rindler, *Spinors and Space-Time*, Vol. 2 (Cambridge University Press, Cambridge), Fig. 6-3, p. 62. This figure demonstrates that vorton structure bears a close resemblance to (a projection of) the twistor.

27. Numerically, $Q_H = m'_\psi \times m_\phi = m_\psi \times m'_\phi = C \times m'_\psi \times m'_\phi$ where C is the largest common factor in $|m_\psi|$ and $|m_\phi|$; *i.e.*, $|m'_\psi|$ and $|m'_\phi|$ are relatively prime. This topic is discussed in Ref. 14.

28. It is of interest to observe that dyality rotation involves an infinitesimal violation of the conservation of charge, which is less restricted than a finite violation: M. B. Voloshin, and L. B. Okun, *Zh. Eksp. Teor. Fiz. Pis'ma Red.*, **28**, 156 (1978) [*JETP Lett.*, **28**, 145 (1978)]; L. B. Okun and Ya. B. Zeldovich, *Phys. Lett. B*, **78**, 597 (1978); A. Yu. Ingnatiev, V. A. Kuzmin, and M. E. Shaposhnikov, *Phys. Lett.*, **84B**, 315 (1979).

29. It is conventionally assumed that the rest mass of the photon is zero ($\lambda\!\!\!^{-}_{\gamma_e} = \infty$), but experimentally it is only known that $\lambda\!\!\!^{-}_{\gamma_e} \gtrsim 3 \times 10^8$ m: E. Fischbach, H. Kloor, R. A. Langel, A. T. Y. Lui, and M. Peredo, *Phys. Rev. Lett.*, **73**, 514 (1994). Earlier refrences for $\lambda\!\!\!^{-}_{\gamma_e}$ are: L. Davis, A. S. Goldhaber and M. M. Nieto, *Phys. Rev. Lett.*, **35**, 1402 (1975); G. V. Chibisov, *Usp. Phys. Nauk*, **119**, (1976) [*Sov. Phys. Usp.*, **19**, 624 (1970)].

30. In the interest of brevity, the word "vortons" will be used to refer to vortons or to a combination of both vortons and antivortons. Context will provide the intended meaning.

31. Although the upward flow of current (lowering negative charge) is the most common cloud-to-ground discharge, this is not an essential feature of the model; it will apply to cloud-to-cloud discharges as well as to cloud-to-ground discharges that lower positive charge to ground.

32. The inverse of this problem, the abrupt creation of a current by beta decay, is treated by J. D. Jackson, *Classical Electrodynamics* (J. Wiley & Sons, Inc., N. Y., 1962), p. 526.

33. This picture of vorton generation also makes it plausible that this model might also explain the phenomenon of bead lightning.[3] However, this intriguing possibility is not explored here.

34. M. A. Uman, *Lightning* (Dover Publication, Inc., N.Y., 1982).

35. Y. T. Lin, M. A. Uman, and R. B. Standler, *J. Geophy. Res.,* **85**, 1571 (1980) postulate that the return stroke is composed of three components: 1) a short duration pulse that produces the fast peak current, 2) a uniform current, and 3) a "corona" current. This model has the peak current flowing at ~ 1 μs after the moment of onset, and yields results in reasonable accord with measurements.

36. A. H. Paxton, R. L. Gardner, and L. Baker, Lightning Return Stroke: A Numerical Calculation of the Optical Radiation, *Lightning Electromagnetics,* R. L. Gardner, Ed. (Hemisphere Publishing Corp., NY, 1990), p. 47.

37. C. R. Holmes, E. W. Szymanski, S. J. Szymanski, and C. B. Moore, *J. Geophys. Res.,* **85**, 7517 (1980), p. 47

38. G. C. Dijkhuis, "Statistics and Structure of Ball Lightning," *Proceedings of the 3rd International Ball Lighting Symposium,* S. Singer, Ed. In press.

39. S. Singer, *op. cit.,* p. 40.

40. *Ibid.,* p. 42.

41. A. J. F. Blair, *Nature*, **243**, 512 (1973).

42. It is also conceivable that lightning produced vortons are excited above the ground state level (thus having $|m_\psi|, |m_\phi| > 1$ and $Q > Q_0$), by the high temperature in the lightning discharge channel, for example. But this possibility is not explored here; as noted in the text, this modification would not significantly affect the physics of this BL model.

43. A detailed description of the process(es) by which the lightning produced vortons (Sec. II D) form a coherent and active BL core is an important topic for future study. Since Sec. II F indicates that it is plausible that every lighting discharge produces

enough vortons to populate numerous BL's, it appears likely that this formation process, going from produced vortons into a coherent BL core, would have a low probability and is the step that makes BL a rare phenomenon. The requisite energy for production is easily available, but the development of coherence is a rare occurrence. To understand this aspect of the phenomenon is quite difficult, therefore, because, like trying to understand "the tails of a curve," it is the improbable processes and reactions that are the most important.

44. Although one expects $n_k = 3$, yielding $3N_v$ normal modes associated with the translational degrees of freedom in a BL, it may be more appropriate to view these degrees of freedom as harmonic oscillators having $k_B T_k$ as their mean energy content (versus the $(1/2)k_B T_k$ for a monatomic gas). This change would remove the factor (1/2) in Eq. (18). However, the excitations of these normal modes can still be characterized by a Maxwell-Boltzmann (or Bose-Einstein) distribution at a temperature T_k. Here again, is an area for future refinements.

45. M. T. Dmitriev, *Zh. Tekh. Fiz.*, **39**, 387 (1969) [*Sov. Phys.—Tech. Phys.*, **14**, 284 (1969)].

46. S. Singer, *op. cit.,* p. 67.

47. H. A. Bethe and E. E. Salpeter, *The Quantum Mechanics of One and Two Electron Atoms* (Academic Press, NY, 1957), p. 285, *et seq.*

48. This local undulation of the Θ_0 of the Dirac sea is what compensates for the apparent charge nonconservation implied by the dyality rotation of the BL. Under normal circumstances, Θ_0 is a fixed value over all space, defined by the quiescent Dirac sea.

49. The amount of energy released by nucleon decay is several hundred times that of a typical nuclear beta decay.

50. By equipartition, the bulk of this core heat energy would end up in excitations of the core polarization, since each vorton would have a large number of such excitations (infinite?) versus the three kinetic degrees of freedom per vorton.

51. The amount of coupling between the kinetic degrees of freedom and the polarization degrees of freedom would (with other factors) determine the relationship between T_s and T_k. Analysis of this relationship is left for future study.

52. C. Kittel, *Introduction to Solid State Physics*, 2nd edn. (John Wiley & Sons, Inc., 1956).

53. J. D. Jackson, *op. cit.,* p. 498.

54. D. Pines, *Elementary Excitations in Solids* (W. A. Benjamin, Inc., New York, 1963).

55. Actually, since BL supports a complicated set of dynamic processes with energy being continually supplied and lost, at best only an approximate state of thermal equilibrium can be expected.

56. D. L. MacAdam, *Color Measurement*, 2nd revised edn. (Springer-Verlag, Berlin, 1985).

57. G. Wyszecki and W. S. Stiles, *Color Science* (John Wiley & Sons Inc., New York, 1966), p. 470.

58. J. D. Cobine, *Gaseous Conductors* (Dover Publications, Inc., 1958).

59. M. Ouellet, *Nature*, **348**, 492 (1990).

60. R. B. Leighton, *Principles of Modern Physics* (McGraw Hill Book Co., Inc., New York, 1959).

61. E. W. Bach, *"UFOs" from the Volcanoes* (Hermitage Publishers, Tenafly, NJ, 1993). While one may not agree with Bach's theoretical speculations, he deserves credit for compiling an extensive and most useful catalogue of observations.

62. As these balls get brighter (higher temperature), they also expand, which can be interpreted as evidence of a higher T_k and its associated kinetic pressure.

63. In fact, it is natural to propose that a "BL" with a small T_k and $\omega \sim \omega_0$ would be the black or gray BL that are occasionally reported. Although this BL could still be coherent, it would have no luminosity, and electromagnetic charge of $\sim 7 \times 10^{-7}$ C would tend to be opaque to impinging electromagnetic radiation with $\lambda < \bar{a}$. Shades

of gray are possible as variations in optical thickness resulting from a variation in the number of vortons in the BL or earth "light."

64. R. C. Jennison, *Nature*, **224**, 895 (1969).

65. W. R. Corliss, *Lightning, Auroras, Nocturnal Lights, and Related Luminous Phenomena* (The Sourcebook Project, Glen Arm, MD, 1982).

66. P. Devereux, *Earth Lights* (Turnstone Press, 1982), p. 19.

67. It is important to observe that independent of temperature this kinetic motion would not be expected to result in significant blackbody radiation at wavelengths shorter than the typical vorton size $\bar{a}$. Hence, with $\bar{a} \sim 1$ cm, the kinetic temperature plays no direct role in BL luminosity.

68. J. D. Jackson, *op. cit.*, p. 364.

69. This calculation uses 0.0156 as the absolute efficiency of a typical (25 W) tungsten bulb: *Handbook of Chemistry and Physics* (The Chemical Rubber Company, Cleveland, Ohio, 1967, 48th Ed.), p. E-132.

70. As one can see from the analysis in Appendix D, the high energy particles emitted in the nucleon decays will carry most of the decay energy to a considerable distance from the BL, significantly reducing local heating.

71. As part of the heat balance, one must account for the fact that a blackbody also absorbs radiation from the environment; a blackbody sphere of area 1500 cm^2 in an environment of $68°F = 20°C = 293$ K will be absorbing ~ 63 W.

72. A. I. Grigorjev, I. D. Grigorjeva, and S. O. Shirjajeva, "Statistical Analysis of the Ball Lightning Properties," in Ref. 5, p. 88.

73. S. Singer, *op. cit.,* p. 30 and p. 70.

74. E. Strand, *Private communication.*

75. The physics of BL entrainment by local ion motion is another area in need of detailed study.

76. G. Joos, *Theoretical Physics*, 3^{rd} ed. (Hafner Publishing Co., New York, 1957), p. 83.

77. P. Devereux, The Ley Hunter, **114**, 3 (1991).

78. Two cases of BL penetrating glass windows are listed by J. R. Powell and D. Finkelstein, *American Scientist,* **58**, 262 (1970). In one case there was no damage, and in the second a hole 28 cm in diameter was melted in the glass. There are numerous other examples given by A. I. Grigor'ev, I. D. Grigor'eva, and S. O. Shiryaeva, *Jour. Sci. Exp.*, **6**, 261 (1992).

79. One expects that positrons from $\mu^+ \rightarrow e^+ + \bar{\nu}_\mu + \nu_e$ would (probably) have less energy than the primary e^+ from Eq. (20). Hence , should the dominant lepton in Eq. (20) be the muon, then the detection range of the 511 keV annihilation line would be expected to be somewhat less.

80. G. E. Brown, *Unified Theory of Nuclear Models and Forces* (North Holland Publishing Co., Amsterdam, 1967).

81. D. E. T. F. Ashby and C. Whitehead, *Nature*, **230**, 180 (1971).

82. It should be noted that the original motivation for the Ashby and Whitehead experiment was to investigate the possibility that BL was due to antimatter annihilation. They subsequently abandoned their hypothesis, D. E. T. F. Ashby, *Private communication.* Ashby and Whitehead's data also tended to refute the (atmospheric) radioactivity theory of M. D. Altschuler, L. L. House, and E. Hildner, *Nature*, **228**, 545 (1970). Another possible source of e^+ associated with thunderstorm activity is the runaway electron hypothesis: C. T. R. Wilson, *Proc. Roy. Soc. A*, **92**, 554 (1916); A. V. Gurevich, G. M. Milikh, and R. Roussel-Dupre, *Phys. Lett. A*, **165**, 463 (1992). It should be noted that the result in which no significant annihilation gamma radiation was found in association with 12 documented nearby lighting discharges [D. Fryberger, "An Experimental Search for Gamma Radiation Associated with Thunderstorm Activity," *Proceedings of the 3rd International Symposium on Ball Lightning*, S. Singer, Ed., in press] tends to refute the hypothesis that runaway electrons (or anything else, for that matter) cause electromagnetic showers beneath thunderstorms. On the other hand, there is revived interest in the runaway electron theory, which might be associated with luminous flashes seen high in the atmosphere

and generally over thunderstorm activity. R. A. Kerr, *Science*, **264**, 1250 (1994). But the X-ray and gamma ray photons generated in electromagnetic showers in the atmosphere above thunderstorms would not be able to penetrate to ground level where the Ashby and Whitehead apparatus was located.

83. G. N. Shah, H. Razdan, C. L. Bhat, and Q. M. Ali, *Nature*, **313**, 773 (1985).

84. W. Cowgill, *Scientific American*, **55**, 389 (1886). This BL was described as "a vivid, dazzling light, which brilliantly illuminated the interior of the house." With such a description, it could exceed the typical 68 W_W BL by an order of magnitude or so, entailing a radioactivity of perhaps 2×10^4 Ci. The distance from the observers to the BL was evidently small, but there is no indication of the duration of the exposure.

85. A. A. Mill , *Nature,* **233**, 131 (1971); S. J. Fleming and M. J. Aitken, *Nature,* **252**, 220 (1974).

86. W. Morris, *Daily Mail*, Letter to Ed. (November 5, 1936); B. L. Goodlett, *J. Inst. Elect. Eng.,* **81**, 1 (1937).

87. M. Stenhoff, *Nature*, **260**, 596 (1976); E. R. Wooding, *ibid.,* **262**, 379 (1976).

88. A. Wittmann, *Nature* **232**, 625 (1971).

89. S. Singer, *op. cit.,* p. 35; W. N. Charman, *op. cit.,* p. 265; K. L. E. Nickel, in Ref. 5, quoting J. Schneider, *Medizinisches vom Gewitterflug am* August 6, 1938. *Thermik* **3**, p. 1920 (1950).

90. M. T. Dmitriev, V. M. Deriugin, and G. A. Kalinkevich, *Zh. Tech. Fiz.,* **42**, 2187 (1972) [*Sov. Phys.-Tech. Phys.,* **17**, 1724 (1973)].

91. Note that this mass differs somewhat from that of Eq. (4) in that the energy due to motion is not included.

92. F. W. Sears, *Thermodynamics, the Kinetic Theory of Gases, and Statistical Mechanics*, 2^{nd} edn. (Addison-Wesley Publishing Co., Inc., Reading, MA, 1953).

93. E. Fermi, *Thermodynamics* (Dover Publications, Inc., New York, 1956), p. 25.

94. H. S. Pruys, R. Engfer, R. Hartmann, E. A. Hermes, H. P. Isaak, F. W. Schlepuetz, U. Sennhauser, W. Dey, K. Hess, H.-J. Pfeiffer, and H. K. Walter, *Nuc. Phys.,* **A352**, 388 (1981).

95. L. G. Porter, J. C. Earnshaw, E. Tielsch-Cassel, J. C. Ahlstrom, and K. Greisen, *NIM*, **87**, 87 (1970).

96. While the I_r can be expected to be proportional the BL radioactivity to $\mathcal{R}_{BL}$, the voltage buildup will not be. As $\mathcal{R}_{BL}$ increases, the local ionization will also increase, proportionately increasing local conductivity. Thus, one can expect that, to a first approximation, these two affects will cancel and the static voltage build-up will be independent of $\mathcal{R}_{BL}$. Thus, we arbitrarily use the gradient 4.5 kV/cm, estimated by Dmitriev[45] and a corona discharge radius of 10 cm.

97. N. P. Bansal and R. H. Doremus *Handbook of Glass Properties* (Academic Press, Inc., Orlando, 1986).